**Figure 4. Development of NS5A-ATeam and SGR-ATeam to enable real-time monitoring of ATP.** (A) Schematic representation of the ATeam and NS5A-ATeam used in this study. ATeam genes were inserted into the 3' region of a HA-NS5A expression vector to generate NS5A-ATeam. The underlined sequences indicate NS5A residues. The insertion site was between residues 2394 and 2395, numbered according to the polyprotein of the HCV JFH-1 isolate. CMV, Cytomegalovirus promoter; CAG, CAG promoter; ATP b.p, ATP binding protein. HA, HA tag. (B) Huh-7 cells were transfected with ATeam and NS5A-ATeam constructs. Forty-eight hours post-transfection, the Venus/CFP ratios of each cell were calculated from fluorescent images acquired with a confocal microscope in the same way as described in the legends for Figure 2. Each plot shows the ratio of individual cells. Horizontal lines represent means. (C) Schematic representation of the SGR and SGR-ATeam plasmids used, with or without the firefly luciferase gene (Fluc). HCV polyproteins are indicated by the open boxes. ATeam genes were inserted into the same site in the NS5A C-terminal region. Bold lines indicate the HCV UTR. EMCV IRES is denoted by the gray bars. Pol I P, Pol I promotor; dC, 5' region of Core gene; Pol I T, Pol I terminator. (D) Replication levels of SGR/luc-AT1.03 in transfected cells were determined by luciferase assay 1–5 days post-transfection. SGR/luc and SGR/luc-GND were used as positive and negative controls, respectively. Values given were normalized for transfection efficiency with luciferase activity determined 24 h post-transfection. All data are presented as means and SD for three independent samples. (E) Huh-7 cells were transfected with constructs encoding NS5A, NS5A-AT1.03, SGR, SGR-AT1.03, SGR/luc or SGR/luc-AT1.03, followed by immunoblotting with anti-NS5B or anti-beta-actin antibody. (F) Cells transfected with constructs encoding NS5A, NS5A-AT1.03, SGR or SGR-AT1.03 were analyzed by immunoblotting with anti-NS5A, anti-NS5B or anti-beta-actin antibodies.
doi:10.1371/journal.ppat.1002561.g004

CFP ratio than the surrounding cytoplasmic region (Figure 5B; middle and lower panels). Although the number of high Venus/ CFP ratios was not consistent between the cells, this phenotype was observed in most of the cells that were replicating SGR-AT1.03 (Figure S3). Such high focal Venus/CFP ratios were not detected in cells replicating SGR-AT1.03$^{RK}$ or in SGR-AT1.03$^{YEMK}$ -replicating cells treated with 2DG and OliA. Thus, foci with a high Venus/CFP ratio apparently represent the presence of high ATP levels at distinct sites in cells replicating HCV RNA. In addition, when a replication-defective polyprotein that extended from NS3 through to the NS5B protein, including NS5A-AT1.03, was expressed, no high Venus/CFP ratio was seen in the cells in spite of the fact that NS5A-AT1.03 was detected in dot-like structures throughout the cytoplasm (Figure S4). These results strongly suggest that the high Venus/CFP ratios observed

using the SGR-ATeam system are associated with the replication of HCV RNA.

To investigate whether the high Venus/CFP ratios of the dot-like structures detected in cells replicating SGR-ATeam are located at the HCV RC, FRET images of SGR-AT1.03-replicating cells were analyzed, followed immunofluorescence analysis of cells fixed and stained with either anti-NS5A or anti-NS3 antibodies (Figure 5C). Confocal fluorescence microscopy at high magnification demonstrated that the high Venus/CFP ratios that were identified in foci of various sizes were co-localized with NS5A and NS3 that were possibly membrane-bound within the cytoplasm of the viral replicating cells. Some of the NS3- or NS5A-labeled proteins that were identified by immunofluorescence were not associated with high Venus/CFP ratios. These results are consistent with previous reports, which demonstrated that only
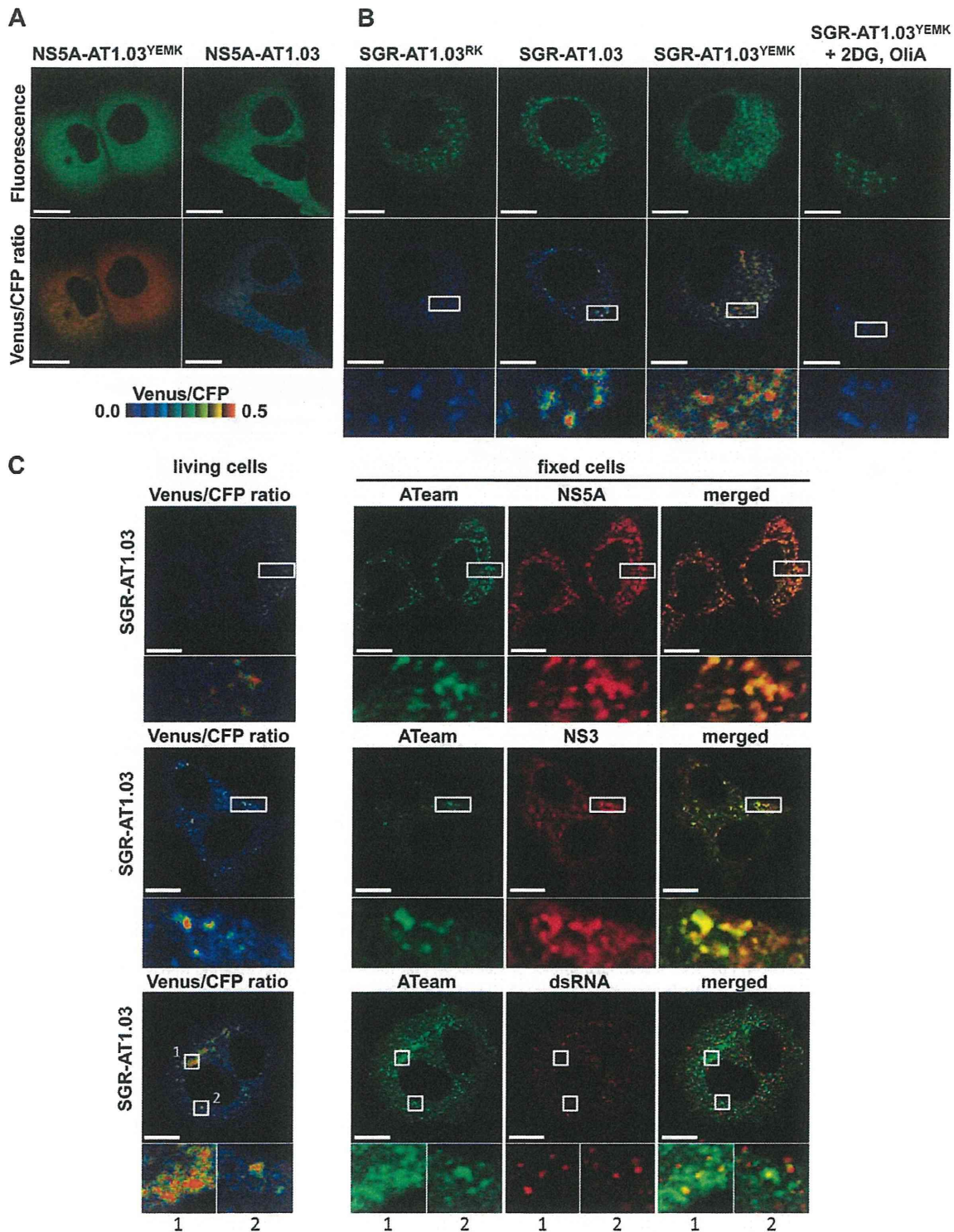
**Figure 5. Visualization of sites of focal accumulation of ATP in cells expressing NS5A-ATeam or SGR-ATeam.** (A) Huh-7 cells were transfected with NS5A-AT1.03 or NS5A-AT1.03$^{YEMK}$. Four days after transfection, the cells were analyzed using spectral imaging (405-nm excitation) of LSM510-META (Carl Zeiss). Images were processed to the CFP channel ($F_{CFP}$) and the Venus channel ($F_{Venus}$) using a linear unmixing algorithm using a reference for each spectrum. The upper panels demonstrate the signal intensity from a spectral channel with maximum intensity and represent the expression pattern of NS5A-ATeam. The lower panels are constructed from FRET ratio images ($F_{CFP}/F_{Venus}$) with pseudocolors. The pseudocolor scale is shown below. Scale bars, 20 µm. (B) Huh-7 cells were transfected with SGR-AT1.03$^{RK}$, SGR-AT1.03 or SGR-AT1.03$^{YEMK}$, and were analyzed in the same

- 663 -

way as described in (A). SGR-AT1.03$^{YEMK}$-transfected cells were treated with 10 mM 2DG and 10 µg/ml OliA just before imaging and were used as a negative control. The upper panels demonstrate the intensity from a spectral channel with maximum intensity and represent the expression pattern of NS5A-ATeam processed from SGR-ATeam. The lower panels indicate square areas within FRET ratio panels magnified five-fold. Scale bars, 20 µm. (C) Cells were fixed after live-cell FRET imaging, and the same cell was analyzed by indirect immunofluorescence staining. Viral proteins were labeled with antibodies against NS5A (upper panels), NS3 (middle panels) and dsRNA (lower panels), which were detected with an Alexa Fluor 555-labeled anti-rabbit or anti-mouse antibody. ATeam panels (green) represent the expression of NS5A-ATeam processed from SGR-ATeam, and NS5A, NS3 or dsRNA panels (red) represent the immunostained signals. Enlarged views of the areas outlined by squares at a five-fold magnification are also shown. Scale bars, 20 µm.

doi:10.1371/journal.ppat.1002561.g005

some of the expressed HCV NS proteins contribute to viral RNA synthesis [27]. To further investigate the relationship between the cellular sites at which there was a high Venus/CFP ratio and HCV RNA replication, double-stranded RNA (dsRNA) was visualized by staining with a specific anti-dsRNA antibody after FRET imaging (Figure 5C). This staining indicated that dsRNA-containing dot-like structures co-localized with structures that displayed high Venus/CFP ratios. Therefore, it is most likely that the dot-like structures with high Venus/CFP ratios that were detected using the SGR-ATeam system reflect the sites of HCV RNA replication or HCV RCs.

Several studies have shown that mitochondria, which play a central role in ATP metabolism, localize to areas near the membranous web, the likely site of HCV RNA replication [28]. We thus compared the subcellular localization of the fluorescence signals detected in cells expressing SGR-ATeam with that of mitochondria that were visualized by staining with Mitotracker. Foci with high Venus/CFP ratios did not colocalize with, but were localized adjacent to mitochondria in cells that were replicating SGR-AT1.03 (Figure S5). This finding might reflect the fact that ATP can be directly supplied from mitochondria to the sites of viral RNA replication in cells.

## Quantification of ATP at putative cytoplasmic sites of HCV RNA replication within cells

Based on the above observations, FRET signals detected within cells expressing SGR-ATeam or NS5A-ATeam can be classified as either signals from distinct dot-like structures, which represent putative subcellular sites of HCV RNA replication, or as signals that are diffuse throughout the cytoplasm. The Venus/CFP emission ratio in individual cells into which NS5A-AT1.03, NS5A-AT1.03$^{YEMK}$, SGR-AT1.03, SGR-AT1.03$^{YEMK}$ or SGR-AT1.03$^{RK}$ was introduced was determined (Figure 6A). Fluorescent signals corresponding to cytoplasmic ATP were identified by subtracting signals at putative sites of viral RNA replication from signals from the cytoplasmic area as a whole. Cytoplasmic Venus/CFP ratios within cells replicating SGR-AT1.03 and SGR-AT1.03$^{YEMK}$ were lower than those in cells expressing NS5A-AT1.03 and NS5A-AT1.03$^{YEMK}$, respectively. Therefore, cytoplasmic ATP levels within HCV RNA-replicating cells were lower than in non-replicating cells. This result is consistent with the findings shown in Figure 1A. The average Venus/CFP ratios at potential sites of viral RNA replication were greater than the corresponding cytoplasmic levels in cells replicating SGR-AT1.03 or SGR-AT1.03$^{YEMK}$. As expected, a significant decrease in Venus/CFP ratios was observed in cells treated with 2DG and OliA.

We next quantified ATP levels within individual cells replicating HCV RNA based on the Venus/CFP ratios obtained. To generate standard curves for this calculation, permeabilized cells expressing NS5A-AT1.03 or NS5A-AT1.03$^{YEMK}$ were prepared by digitonin treatment, followed by the addition of defined concentrations of ATP and subsequent FRET analysis [29,30]. As shown in Figure 6B, under these experimental conditions, baseline Venus/CFP ratios of approximately 0.1 were detected in the absence of exogenous ATP, and Venus/CFP ratios were observed to increase

linearly with increasing ATP concentration. The standard curves thus obtained can be used to estimate the ATP concentrations of unknown samples in which a particular ATeam containing an ATP probe at the C terminus of HCV NS5A, such as NS5A-ATeam or SGR-ATeam, have been introduced. Based on the fluorescent signal obtained in cells replicating SGR-ATeam, as well as in cells expressing NS5A-ATeam, the ATP concentration at putative sites of HCV RNA replication was estimated to be ~5 mM in the experiments shown in Figures 5A and 5B (average value of putative replication sites; 4.8 mM). After subtraction of the ATP that was localized at the HCV replication sites, the ATP concentration of HCV-replicating SGR cells (~1 mM) was found to be approximately half that observed in parental non-replicating cells (~2 mM)(average values in SGR and parental cells; 0.8 mM and 2.2 mM, respectively). To our knowledge, this is the first experiment in which ATP levels were estimated inside living cells during viral genome replication.

Figures 5 and 6A demonstrate changes in ATP concentrations at distinct sites in cells undergoing HCV RNA replication. Finally, we determined the effect of the PSI-6130 inhibitor of HCV replication on the change in subcellular ATP concentration in cells following introduction of SGR-AT1.03, SGR-AT1.03$^{RK}$ or NS5A-AT1.03 (Figure 6C). In general, nucleoside analogue inhibitors of viral replication prevent RNA/DNA synthesis by chain termination immediately after addition to infected cells [23]. Indeed, as shown in Figure 3, a decrease in ATP consumption was detected even following a PSI-6130 treatment period as short as 15 min of permeabilized HCV replicon cells. We therefore analyzed and estimated ATP levels in cells in the presence of PSI-6130 for 10 min and 2 h. ATP concentrations at putative sites of viral RNA replication, as well as cytoplasmic ATP levels, were higher in SGR-AT1.03-replicating cells in the presence of 0.1–5 µM PSI-6130 for 10 min compared to the same cells without inhibitor treatment or to NS5A-AT1.03-expressing cells. A dose-dependent PSI-6130-induced increase in ATP levels at the putative replication sites was observed under the condition used. By treatment with PSI-6130 for 2 h, the ATP levels at putative replication sites were significantly lower than those without inhibitor treatment in SGR-AT1.03-replicating cells. The cytoplasmic ATP levels were similar with or without 2-h treatment (Figure 6C). In HCV SGR-ATeam cells treated with PSI-6130 for 3 days, HCV RNA replication was dramatically inhibited by greater than 90% with no observed cytotoxicity (Figure S6) and, as expected, little or no high Venus/CFP signal was detected anywhere in the cells (data not shown). We adapted the ATeam system to monitor ATP in HCV RNA replicating cells and found increased ATP levels at the putative subcellular sites of the viral replication. Findings obtained from experiments using the viral polymerase inhibitor strongly suggest that changes in ATP concentrations at the distinct sites observed depend on the viral RNA replication.

## Discussion

This paper is the first to demonstrate changes in ATP within cells during viral genome replication. ATP requirements during
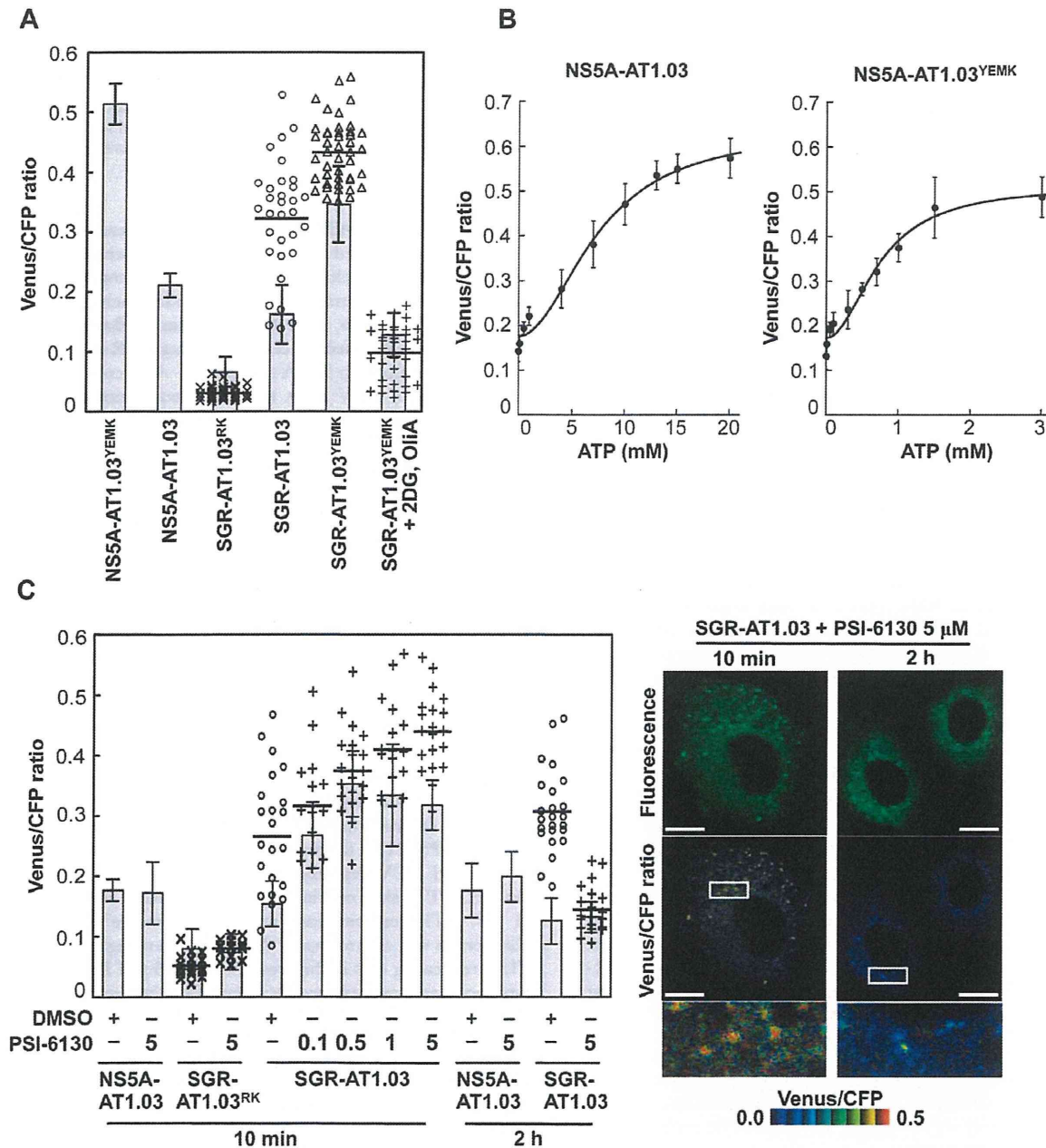
**Figure 6. Estimation of ATP levels at possible sites of HCV RNA replication in living cells.** (A) Venus/CFP emission ratios were calculated from images of CFP and Venus channels in individual cells for each group. Bar- and dotted graphs indicate ratios within the cytoplasm and ratios for dot-like structures, respectively, in the same cells, as shown in Figures 5A and 5B. Data in bar graphs are indicated as means and SD. Horizontal lines in the dot graphs denote means from at least three independent cells. Values in the cytoplasm of cells transfected with NS5A-AT1.03$^{YEMK}$ and SGR-AT1.03$^{YEMK}$ were statistically significant ($p<0.05$) as evaluated using the Student's $t$-test. (B) Calibration of NS5A-ATeam in cells under semi-intact conditions. Cells were transfected with NS5A-AT1.03 and NS5A-AT1.03$^{YEMK}$, respectively. Forty-eight hours later, the cells were permeabilized, followed by addition of known concentrations of ATP. FRET analyses were performed as described in Figure 5A. Each trace represents mean with SD of at least six independent cells. Plots were fitted with Hill equations with a fixed Hill coefficient of 2; $R = (R_{max} - R_{min}) \times [ATP]^2/([ATP]^2 + Kd^2) + R_{min}$, where $R_{max}$ and $R_{min}$ are the maximum and minimum fluorescence ratios, respectively. $Kd$ is the apparent dissociation constant. R values were 0.994 and 0.986 for NS5A-AT1.03 and NS5A-AT1.03$^{YEMK}$, respectively. (C) Cells were transfected with NS5A-AT1.03, SGR-AT1.03$^{RK}$ or SGR-AT1.03. The cells were then treated with PSI-6130 at indicated concentrations (μM) for 10 min or 2 h, and were analyzed as described in (A). Values in the cytoplasm of cells transfected with SGR-AT1.03 with and without PSI-6130 treatment were statistically significant ($p<0.05$ for control versus 0.1 or 1 μM PSI-6130, $p<0.01$ for control versus 0.5 or 5 μM PSI-6130) as evaluated using the Student's $t$-test. Representative cells treated with 5 μM PSI-6130 are shown in the right panel. The lower panel is a five-fold magnification of the boxed area. Scale bars, 20 μm.
doi:10.1371/journal.ppat.1002561.g006

- 665 -

the virus lifecycle have been studied for years. Several key steps during the viral life cycle, such as genome synthesis, require high-energy phosphoryl groups. For instance, it has been shown that ATP is required for the formation of a preinitiation complex for de novo RNA synthesis by RdRp of flaviviruses [31]. Transcriptional initiation and RNA replication by influenza virus RdRp are functional in an ATP-dependent fashion [32,33]. An ATP requirement of viral helicase activities has also been reported [34]. Furthermore, it has been demonstrated that ATP is involved in the assembly and/or release of viral structural proteins possibly via interaction with ATP-dependent chaperones [35,36]. However, it has been controversial as to whether ATP can be concentrated in particular subcellular compartment(s) in infected cells during viral replication. One of the underlying reasons for this controversy may be that a method by which cellular ATP levels can be determined, apart from examination of ATP levels in cellular extracts in the steady-state, has been lacking [37]. Recently Imamura et al. established FRET-based indicators, known as ATeams, for ATP quantification, and have shown that the use of ATeams enables the monitoring of ATP levels in real-time in different cellular compartments within individual cells [2].

In this study, in order to visualize and monitor ATP levels in living cells during replication of the viral genome, we first introduced the original ATeam-expressing plasmids into cells and found that cytoplasmic ATP levels in cells undergoing HCV genotype 1b and 2a RNA replication were lower than those in cured or parental cell lines (Figures 2 and S2). These results agree with the results of CE-TOF MS analysis (Figure 1) and the ATP consumption assay (Figure 3). It is therefore likely that ATP is actively consumed in cells during viral RNA replication, resulting in reduced levels of ATP in the cytoplasm. Furthermore, NS5A-ATeam fusion constructs, in which the ATeam gene was introduced into the C-terminal end of the NS5A coding region, and SGR-ATeam constructs containing a HCV JFH-1-derived subgenomic replicon within the NS5A-ATeam fused sequence as described above, were engineered (Figure 4). The results obtained using several ATeam fusion constructs with different affinities for ATP indicated that NS5A-ATeam fusion constructs can be used as FRET-based ATP indicators, and that the ATeam-tagged HCV replicons are capable of transient replication of viral RNA (Figure 4). It is interesting that our experiment using a SGR-ATeam construct provides evidence for the formation of ATP-enriched foci within cells that support HCV RNA replication (Figures 5 and 6). FRET-signal detection followed by indirect immunofluorescence allowed us to visualize co-localization of viral proteins as well as dsRNA at sites of ATP accumulation in cells (Figure 5), suggesting that these membrane-associated ATP-enriched foci likely represent sites of HCV RNA replication in transient replication assays.

Attempting to precisely quantify ATP within individual cells or particular intracellular compartments is a very challenging process. The luciferin-luciferase reaction has been utilized to monitor cellular ATP levels by measuring the released photon count during catalysis of bioluminescent oxidation by firefly luciferase. A previous study based on the luciferin-luciferase assay estimated basal cytoplasmic ATP levels at ~1.3 mM, which increased to ~5 mM during apoptotic cell death [38]. However, the results obtained were likely influenced by cellular levels of luciferase and other assay components, as well as by the pH of the cells. In this study, we describe quantification of ATP in human hepatoma Huh-7 cells undergoing HCV RNA replication using SGR-ATeam technology. Although ATP requirements during the lifecycles of various viruses have been studied for years, the use of ATeam technology enabled us, for the first time, to evaluate ATP

concentrations at sites of viral replication within living cells. We here demonstrate that ATP concentrations at these putative subcellular sites of HCV RNA replication approach ~5 mM (Figure 6). This ATP level is as high as that observed during apoptotic processes such as caspase activation and DNA fragmentation, even though the latter ATP level was determined using a different assay system [38]. Considering that these apoptotic events were not observed at basal ATP levels [38], replication of the viral genome likely also requires high concentrations of cellular ATP. It should be noted that, in contrast to the fluorescent reporter system traditionally used to calculate the ATP/ADP ratio [39], the bacterial epsilon subunit used in ATeam is highly specific for ATP, but not for other nucleotides such as ADP, CTP, GTP or UTP [2,3]. In evaluating the effect of the HCV polymerase inhibitor on changes in the subcellular ATP concentration in cells replicating SGR-ATeam, an increase in ATP concentration was observed both at putative replication sites and in the cytoplasm of SGR-AT1.03-replicating cells in the presence of PSI-6130 for 10 min (Figure 6C). By contrast, 2-h treatment with the inhibitor resulted in reduction of ATP levels at putative replication sites in the replicon cells. Although the result of the experiment with 10-min treatment may be somewhat unexpected, it might possibly be explained by the following hypothesis. PSI-6130 began to inhibit viral RNA synthesis, leading to a decrease in ATP consumption. Since a mechanism for ATP transport mediated by host cell and/or viral factor(s) is still active during this time period, the ATP level at the replication sites should be increased compared to that during active replication. Higher levels of metabolic intermediates for glyconeogenesis as well as for glycolysis in HCV-infected cells compared to non-infected cells as determined via metabolome analysis (data not shown) may also be implicated in the increased ATP levels at the initial stage of inhibition of HCV replication. It is likely that active consumption of ATP caused by HCV replication and ATP transportation into the replication sites would lead to reduction of cytoplasmic ATP level. Such a change in ATP balance may result in induction of ATP generation and increase in certain metabolic intermediates related to glucose metabolism. These metabolome responses are supposed to maintain in short-term (10 min) treatment with PSI-6130. Thus, inhibition of HCV RNA replication by PSI-6130 under the conditions used may lead to increase in the cytoplasmic ATP level. It is likely that these metabolome responses were not observed after the longer-term (2 h) treatment presumably because the viral replication was inhibited by the inhibitor for a sufficient period of time. Further study is required to address the molecular mechanism underlying change in ATP balance caused by HCV replication and the viral inhibitors.

The mechanism by which ATP accumulates at potential sites of HCV RNA replication remains unclear. We have previously demonstrated that creatine kinase B (CKB), which is an ATP-generating enzyme and maintains cellular energy stores, accumulates in the HCV RC-rich fraction of viral replicating cells [22]. Our earlier results suggest that CKB can be directed to the HCV RC via its interaction with the HCV NS4A protein and thereby functions as a positive regulator for the viral replicase by providing ATP [22]. One may hypothesize that recruitment of the ATP generating machinery into the membrane-associated site, through its interaction with viral proteins comprising the RC, is at least in part linked with elevated concentrations of ATP at a particular site. Through our preliminary study, however, subcellular ATP distribution was not changed significantly in replicon cells where HCV RNA replication was reduced ~50% by siRNA-mediated knockdown of the CKB gene (data not shown). Another possibility

may be implication of communication between mitochondria and membrane-enclosed structures of HCV RC in ATP transport through membrane-to-membrane contact. As indicated in Figure S5, putative sites of the viral RNA replication with high Venus/CFP ratios were mainly localized proximal to mitochondria. Studies are ongoing to understand the mechanism(s) underlying this phenomenon, as well as to determine if changes in ATP levels at intracellular sites supporting replication might also be observed for other RNA or DNA viruses.

In summary, we have used a FRET-based ATP indicator called ATeam to monitor ATP levels in living cells where viral RNA replicates by designing HCV replicons harboring wild-type or mutated ATeam probes inserted into the C-terminal domain of NS5A. We evaluated changes in ATP levels during HCV RNA replication and demonstrated elevated ATP levels at putative sites of replication following detection of FRET signals, which appeared as dot-like foci within the cytoplasm. The ATeam system may become a powerful tool in microbiology research by enabling determination of subcellular ATP localization in living cells infected or associated with microbes, as well as investigation of the regulation of ATP-dependent processes during the lifecycle of various pathogens.

## Materials and Methods

### Chemicals

PSI-6130 (β-$_D$-2'-Deoxy-2'-fluoro-2'-C-methylcytidine) and recombinant human IFN-alpha2b were obtained from Pharmasset Inc. (Princeton, NJ) [23,24] and Schering-Plough (Kenilworth, NJ), respectively. OliA and 2DG were purchased from Sigma-Aldrich (St. Louis, MO). ATP used in this study was complexed with equimolar concentrations of magnesium chloride before use in the experiments.

### Plasmids

The construction of the ATeam plasmids pRSET-AT1.03, pRSET-AT1.03$^{YEMK}$ and pRSET-AT1.03$^{R122K/R126K}$, which express wild-type ATeam (AT1.03), as well as a high-affinity mutant (AT1.03$^{YEMK}$) and a non-binding mutant (AT1.03$^{RK}$), has been previously described [2]. pHH/SGR-Luc (also termed SGR/luc) contains cDNA of a subgenomic replicon of HCV JFH-1 isolate (genotype 2a; [14]) with firefly luciferase flanked by the Pol I promoter and the Pol I terminator, yielding efficient RNA replication upon DNA transfection [26]. pHH/SGR-Luc/GND (also termed SGR/luc-GND), in which a point mutation of the GDD motif of the NS5B was introduced in order to abolish RNA-dependent RNA polymerase activity, was used as a negative control. pHH/SGR (also termed SGR) was created by deleting the luciferase gene in pHH/SGR-Luc. To generate a series of SGR-ATeam plasmids, wild-type or mutant ATeam genes were inserted into pHH/SGR-Luc or pHH/SGR at the Xho I site of NS5A (between amino acids 418 and 419) [25]. The ATeam genes were also inserted into the same site of pCAGNS5A, which contains the NS5A gene of JFH-1 downstream of the CAG promoter and hemagglutinin (HA) tag [26], yielding NS5A-ATeam plasmids. To generate a plasmid expressing NS3-NS5B-AT1.03 under the control of the CAG promoter, a DNA fragment containing the coding region of NS3/NS4A/NS4B/NS5A-AT1.03/NS5B of SGR/luc-ATeam was inserted into the pCAGGS vector [40]. Exact cloning strategies are available upon request.

### Cell culture and plasmid transfection

Human hepatoma Huh-7 cells were propagated in Dulbecco's modified Eagle's medium (DMEM) supplemented with 10% fetal calf serum (FCS) as well as minimal essential medium non-essential amino acid (MEM NEAA)(Invitrogen, Carlsbad, CA) in the presence of 100 units/ml of penicillin and 100 μg/ml of streptomycin. The Huh-7-derived cell lines JFH-1/4-1 and JFH-1/4-5, which support replication of SGR RNA of HCV JFH-1 (genotype 2a) and NK5.1/0-9, which carries the SGR RNA of Con1 NK5.1 (genotype 1b), were cultured and maintained under previously described conditions [15]. DNA transfection was performed using a TransIT-LT1 transfection reagent (Takara, Shiga, Japan) in accordance with the manufacturer's instructions.

### CE-TOF MS analysis

Huh-7 cells were mock-infected or infected with HCVcc derived from a wild-type JFH-1 isolate at a multiplicity of infection of 1. When most cells had become virus positive, as confirmed by immunofluorescence, with no observable cell damage at 9 days post-infection, equal amounts of cells with and without HCV infection were scraped with MeOH including 10 μM of an internal standard after washing twice with 5% mannitol solution. Replicon cells (JFH-1/4-5) that were cultured in the absence of G418 for 2 days were harvested and prepared as above. The extracts were mixed with chloroform and water, followed by centrifugation at 2,300× g for 5 min at 4°C, The upper aqueous layer was centrifugally filtered through a 5-kDa cutoff filter to remove proteins. The filtrate was lyophilized and dissolved in water, then subjected to CE-TOF MS analysis. CE-TOF MS experiments were performed using an Agilent CE-TOF MS system (Agilent Technologies, Waldbronn, Germany) as described previously [41].

### ATP consumption assay

The ATP consumption assay using permeabilized replicon cells was carried out as previously described [13,22] with slight modifications, so that it was unnecessary to add either exogenous phosphocreatine or creatine phosphokinase to minimize ATP reproduction in cells. Cells (2×10$^6$) cultured in the presence or absence of PSI-6130 for 72 h were treated with 5 μg Actinomycin D/ml, followed by trypsinization and 3 washes with cold buffer B (20 mM HEPES-KOH [pH 7.7], 110 mM potassium acetate, 2 mM magnesium acetate, 1 mM EGTA, and 2 mM dithiothreitol). The cells were permeabilized by incubation with buffer B containing 50 μg/ml digitonin for 5 min on ice and the reaction was stopped by washing 3 times with cold buffer B. The permeabilized cells (1×10$^5$) were resuspended with 100 μl buffer B containing 5 μM ATP, GTP, CTP, and UTP, 20 μM MgCl$_2$, and 5 μg/ml Actinomycin D. After incubation at 27°C for 15 min, samples were centrifuged, and 20 μl of the supernatant was then mixed with 5 μl of 5× passive lysis buffer (Promega, Madison, WI). The ATP level was determined using a CellTiter-Glo Luminescent cell viability assay system (Promega). All assays were performed at least in triplicate.

### Live cell microscopy

Plasmids carrying the ATP indicators were transfected at 48 h (ATeam and NS5A-ATeam) or 4 days (SGR-ATeam) before imaging of the cells. One day before imaging, the cells were seeded onto 30-mm glass-bottomed dishes (AGC Techno Glass, Chiba, Japan) at about 60% confluency. For imaging, the cells were maintained in phenol red-free DMEM containing 20 mM HEPES-KOH [pH 7.7], 10% FCS and MEM NEAA.

Two kinds of confocal microscopies were used to perform the FRET analysis in this study as follows. Since the ways of acquisition of each spectrum were quite different between the two microscopies, differences in the values of the Venus/CFP ratios in different

experiments were observed. In Figures 2, 4B and S2, cells were imaged using a confocal inverted microscope FV1000 (Olympus, Tokyo, Japan) equipped with an oil-immersion 60× Olympus UPlanSApo objective (NA = 1.35). Cells were maintained on the microscope at 37°C with a stage-top incubation system (Tokai Hit, Shizuoka, Japan). Cells were excited by a 405-nm laser diode, and CFP and Venus were detected at 480–500 nm and 515–615 nm wavelength ranges, respectively. In the analysis shown in Figures 5, 6, S3, S4 and S5, FRET images were obtained using a Zeiss LSM510 Meta confocal microscope with an oil-immersion 63× Zeiss Plan-APOCHROMAT objective (NA = 1.4)(Carl Zeiss, Jena, Germany). Cells were maintained on the microscope at 37°C with a continuous supply of a 95% air and 5% $CO_2$ mixture using a XL-3 incubator (Carl Zeiss). Cells were excited by a 405-nm blue diode laser, and emission spectra of 433–604 nm wavelength range were obtained using an equipped scanning module (META detector) [42,43]. Images were computationally processed by a linear unmixing algorithm using the reference spectrum of CFP and Venus, which were obtained from individual fluorescence-expressing cells. All image analyses were performed using MetaMorph (Molecular Devices, Sunnyvale, CA). Fluorescence intensities of cytoplasmic areas in NS5A-ATeam transfected cells were calculated by subtraction of the signal intensities of the nucleus from the signal intensities of the whole cell, which was standardized by the area of the corresponding cytoplasmic region. Fluorescence intensities of cytoplasmic areas and at dot-like structures corresponding to the putative viral replicating sites in SGR-ATeam-transfected cells were measured and calculated as follows. All pixels above CFP intensity levels of 100–200 were selected. The positions of dot-like structures were then determined by examining areas greater than $0.5 \times 10^{-12}$ square meters and the intensity of each dot was measured. The fluorescence intensity of the cytoplasmic area, excluding that of the putative viral replicating sites in each cell, was calculated by subtraction of the signal intensities of the nucleus and the dot-like structures, as determined above, from the signal intensity of the whole cell, which was standardized by the area of the corresponding cytoplasmic region. Each Venus/CFP emission ratio was calculated by dividing pixel-by-pixel a Venus image with a CFP image.

To investigate the relationship between Venus/CFP ratios and ATP concentrations in cells, calibration procedures were performed according to previous reports [29,30]. Huh-7 cells were transfected with NS5A-AT1.03 or NS5A-AT1.03$^{YEMK}$. Forty-eight hours later, the cells were permeabilized by incubation with buffer B containing 50 μg/ml digitonin for 5 min at room temperature. The reaction was stopped by washing 3 times with buffer B, followed by the addition of known concentrations of ATP in warmed medium for imaging. FRET analysis, with calibration of the signal intensity in the cytoplasm of each cell, was performed as described above. Plots were fitted with Hill equations with a fixed Hill coefficient of 2; $R = (R_{max} - R_{min}) \times [ATP]^2 / ([ATP]^2 + Kd^2) + R_{min}$, where $R_{max}$ and $R_{min}$ are the maximum and minimum fluorescence ratios, respectively and $Kd$ is the apparent dissociation constant.

To analyze the effect of an inhibitor against HCV NS5B polymerase, the medium for the cells replicating SGR-ATeam was changed to medium containing various concentrations of PSI-6130. After 10-min incubation at 37°C under a continuous supply of 95% air and 5% $CO_2$, fluorescence intensities of cytoplasmic areas and at dot-like structures were determined as described above. Medium containing 0.01% DMSO was used as a negative control.

To visualize mitochondria, MitoTracker Red CMXRos (Molecular Probes, Eugene, OR) was added to the culture medium to a final concentration of 100 nM, incubated for 15 min at 37°C and the cells were then washed twice with phosphate buffered saline (PBS) before FRET analysis of living cells. Images were computationally processed as described above. The reference spectrum of MitoTracker Red CMXRos was obtained from stained parental, non-transfected, Huh-7 cells.

## Indirect immunofluorescence

Cells expressing SGR-ATeam were cultured in 30-mm glass-bottomed dishes with an address grid on the coverslip (AGC Techno Glass). After FRET analysis of living cells as described above, the cells were fixed with 4% paraformaldehyde at room temperature for 30 min. After washing with PBS, the cells were permeabilized with PBS containing 0.3% Triton X-100 and individually stained with a rabbit polyclonal antibody against NS3 [44], an anti-NS5A antibody [45], or a mouse monoclonal antibody against dsRNA antibody (Biocenter Ltd., Szirak, Hungary) [46]. The fluorescent secondary antibody used was Alexa Fluor 555-conjugated anti-rabbit- or anti-mouse IgG (Invitrogen). The cells were imaged using a Zeiss LSM510 Meta confocal microscope with an oil-immersion 63× Zeiss Plan-APOCHROMAT objective (NA = 1.4). For dual-color imaging, the ATeam signal was excited with the 488-nm laser line of an argon laser and Alexa Fluor 555 was excited with a 543-nm HeNe laser under MultiTrack mode. Emission filters with a 505- to 530-nm band-pass and 560-nm-long pass filter were used.

## Luciferase assay

Huh-7 cells transfected with SGR/luc or SGR/luc-ATeam were harvested at different time points after transfection (Figure 4D) or at 3 days after treatment with PSI-6130 (Figure S6) and lysed in passive lysis buffer (Promega). To monitor HCV RNA replication, the luciferase activity in cells was determined using a Luciferase Assay system (Promega). All assays were performed at least in triplicate.

## MTT assay

Cell viability was assessed using the Cell Proliferation Kit II (Roche, Indianapolis, IN) according to the manufacturer's instructions. The kit measures mitochondrial dehydrogenase activity, which is used as a marker of viable cells, using a colorimetric sodium3′-[1(-phenylaminocarbonyl)-3,4-tetrazolium]-bis(4-methoxy-6-nitro)benzene sulfonic acid hydrate (MTT) assay.

## Quantification of HCV RNA

HCV RNA copies in the replicon cells with or without PSI-6130 treatment were determined using the real-time detection reverse transcription polymerase chain reaction (RTD-PCR) described previously [47] with the ABI Prisom 7700 sequence detector system (Applied Biosystems Japan, Tokyo, Japan).

## Western blotting

The proteins were transferred onto a polyvinylidene difluoride membrane (Immobilon; Millipore, Bedford, MA) after separation by SDS-PAGE. After blocking, the membranes were probed with a rabbit polyclonal anti-NS5A antibody [44], a rabbit polyclonal anti-NS5B antibody (Chemicon, Temecula, CA), or a mouse polyclonal anti-beta-actin antibody (Sigma-Aldrich), followed by incubation with a peroxidase-conjugated secondary antibody and visualization with an ECL Plus Western blotting detection system (GE Healthcare, Buckinghamshire, UK).

## Supporting Information

**Figure S1 ATP Levels in HCV replicon cells and parental Huh-7 cells determined by CE-TOF MS.** ATP metabolites in Huh-7 cells and JFH-1/4-5 cells were measured by

- 668 -

CE-TOFMS. The values of each measurement are shown at left. The right graph shows means with SD of the data at left. Open bar; Huh-7 cells, gray bar; JFH-1/4-5 cells.
(TIF)

**Figure S2   Cytoplasmic ATP levels in HCV replicon cells and IFN-treated cells.** (Left) The HCV replicon cells JFH-1/4-1, JFH-1/4-5 (genotype 2a) and NK5.1/0-9 (genotype 1b), and parental Huh-7 cells were cultured for 72 h in the absence or presence of 1,000 IU/ml IFN-alpha. Forty-eight hours after transfection with AT1.03, the Venus/CFP emission ratio of each cell was calculated from fluorescent images acquired with the confocal microscope FV1000. All data are presented as means and SD for at least 10 independent cells. (Right) HCV RNA titers in cells corresponding to the left panel were determined using real-time quantitative RT-PCR. Data are presented as means and SD for three independent samples. NTD indicates not detected.
(TIF)

**Figure S3   Increase in ATP-enriched dot-like structures in cells replicating SGR-ATeam.** Huh-7 cells were transfected with SGR-AT1.03, and analyzed in the same way as described in the legends for Figures 5A and 5B. The lower four panels are five-fold magnifications of the boxed areas in independent cells. Scale bars, 40 μm.
(TIF)

**Figure S4   Visualization of the ATP level in cells expressing replication-defective HCV polyprotein.** (A) A schematic representation of the NS3-NS5B-AT1.03 plasmid is shown. The HCV polyprotein is indicated by the open boxes. The ATeam gene was inserted into the same site as that for NS5A-ATeam and SGR-ATeam insertion as indicated in the legend for Figure 4A. CAG, CAG promoter. (B) Cells transfected with constructs encoding NS5A, NS5A-AT1.03, NS3-NS5B-AT1.03, SGR or SGR-AT1.03 were analyzed by immunoblotting with anti-NS5A, anti-NS5B or anti-beta-actin antibodies. (C) Huh-7 cells were transfected with NS3-NS5B-AT1.03, and analyzed in the same way as described in the legends for Figures 5A and 5B. The upper panel (Fluorescence) demonstrates signal intensity from a spectral channel with maximum intensity and represents the expression pattern of NS5A-ATeam processed from NS3-NS5B-AT1.03. The lower panels (Venus/CFP ratio) indicate the FRET

ratio and a five-fold magnification of the boxed area. Scale bar, 20 μm.
(TIF)

**Figure S5   Relationship between ATP-enriched dot-like structures and mitochondria.** Huh-7 cells replicating SGR-AT1.03 (right panels) and parental cells (left panel) were analyzed. Active mitochondria were labeled with MitoTracker Red CMXRos in living cells, and were analyzed in the same way as described in the legends for Figures 5A and 5B, using a reference for the MitoTracker spectrum. The lowest panels of SGR-ATeam cells indicate five-fold magnifications of the boxed areas. Scale bars, 20 μm.
(TIF)

**Figure S6   Inhibitory effect of PSI-6130 on HCV RNA replication.** (A) Replication levels of SGR/luc-AT1.03 RNA in transfected cells were determined by luciferase assay 3 days after treatment with PSI-6130 at the indicated concentrations (μM). The values shown were normalized for transfection efficiency with luciferase activity determined 24 h post-transfection. All data are presented as means and SD for three independent samples. (B) Cell viability was assessed using the MTT assay.
(TIF)

## Author Contributions

Conceived and designed the experiments: T. Ando, H. Imamura, T. Wakita, T. Suzuki. Performed the experiments: T. Ando, H. Aizaki. Analyzed the data: T. Ando, H. Imamura, T. Watanabe, T. Wakita, T. Suzuki. Contributed reagents/materials/analysis tools: H. Imamura, R. Suzuki, H. Aizaki. Wrote the paper: T. Ando, T. Suzuki.

## References

1. Ranji A, Boris-Lawrie K (2010) RNA helicases: Emerging roles in viral replication and the host innate response. RNA Biol 7: 775–787.
2. Imamura H, Nhat KP, Togawa H, Saito K, Iino R, et al. (2009) Visualization of ATP levels inside single living cells with fluorescence resonance energy transfer-based genetically encoded indicators. Proc Natl Acad Sci U S A 106: 15651–15656.
3. Kato-Yamada Y, Yoshida M (2003) Isolated epsilon subunit of thermophilic F1-ATPase binds ATP. J Biol Chem 278: 36013–36016.
4. Iino R, Murakami T, Iizuka S, Kato-Yamada Y, Suzuki T, et al. (2005) Real-time monitoring of conformational dynamics of the epsilon subunit in F1-ATPase. J Biol Chem 280: 40130–40134.
5. Yagi H, Kajiwara N, Tanaka H, Tsukihara T, Kato-Yamada Y, et al. (2007) Structures of the thermophilic F1-ATPase epsilon subunit suggesting ATP-regulated arm motion of its C-terminal domain in F1. Proc Natl Acad Sci U S A 104: 11233–11238.
6. Bartenschlager R, Sparacio S (2007) Hepatitis C virus molecular clones and their replication capacity in vivo and in cell culture. Virus Res 127: 195–207.
7. Pezacki JP, Singaravelu R, Lyn RK (2010) Host-virus interactions during hepatitis C virus infection: a complex and dynamic molecular biosystem. Mol Biosyst 6: 1131–1142.
8. Suzuki T, Ishii K, Aizaki H, Wakita T (2007) Hepatitis C viral life cycle. Adv Drug Deliv Rev 59: 1200–1212.
9. Cai Z, Liang TJ, Luo G (2004) Effects of Mutations of the Initiation Nucleotides on Hepatitis C Virus RNA Replication in the Cell. J Virol 78: 3633–3643.
10. Moradpour D, Penin F, Rice CM (2007) Replication of hepatitis C virus. Nat Rev Microbiol 5: 453–463.
11. Dumont S, Cheng W, Serebrov V, Beran RK, Tinoco I, Jr., et al. (2006) RNA translocation and unwinding mechanism of HCV NS3 helicase and its coordination by ATP. Nature 439: 105–108.
12. Frick DN (2007) The hepatitis C virus NS3 protein: a model RNA helicase and potential drug target. Curr Issues Mol Biol 9: 1–20.
13. Miyanari Y, Hijikata M, Yamaji M, Hosaka M, Takahashi H, et al. (2003) Hepatitis C virus non-structural proteins in the probable membranous compartment function in viral genome replication. J Biol Chem 278: 50301–50308.
14. Wakita T, Pietschmann T, Kato T, Date T, Miyamoto M, et al. (2005) Production of infectious hepatitis C virus in tissue culture from a cloned viral genome. Nat Med 11: 791–796.
15. Miyamoto M, Kato T, Date T, Mizokami M, Wakita T (2006) Comparison between subgenomic replicons of hepatitis C virus genotypes 2a (JFH-1) and 1b (Con1 NK5.1). Intervirology 49: 37–43.
16. Mankouri J, Tedbury PR, Gretton S, Hughes ME, Griffin SD, et al. (2010) Enhanced hepatitis C virus genome replication and lipid accumulation mediated by inhibition of AMP-activated protein kinase. Proc Natl Acad Sci U S A 107: 11549–11554.
17. Nakashima K, Takeuchi K, Chihara K, Hotta H, Sada K (2011) Inhibition of hepatitis C virus replication through adenosine monophosphate-activated protein kinase-dependent and -independent pathways. Microbiol Immunol 55: 774–782.

- 669 -

18. Nagai T, Ibata K, Park ES, Kubota M, Mikoshiba K, et al. (2002) A variant of yellow fluorescent protein with fast and efficient maturation for cell-biological applications. Nat Biotechnol 20: 87–90.
19. Appleby TC, Anderson R, Fedorova O, Pyle AM, Wang R, et al. (2011) Visualizing ATP-dependent RNA translocation by the NS3 helicase from HCV. J Mol Biol 405: 1139–1153.
20. Cheng W, Arunajadai SG, Moffitt JR, Tinoco I, Jr., Bustamante C (2011) Single-base pair unwinding and asynchronous RNA release by the hepatitis C virus NS3 helicase. Science 333: 1746–1749.
21. Beran RK, Lindenbach BD, Pyle AM (2009) The NS4A protein of hepatitis C virus promotes RNA-coupled ATP hydrolysis by the NS3 helicase. J Virol 83: 3268–3275.
22. Hara H, Aizaki H, Matsuda M, Shinkai-Ouchi F, Inoue Y, et al. (2009) Involvement of creatine kinase B in hepatitis C virus genome replication through interaction with the viral NS4A protein. J Virol 83: 5137–5147.
23. Ma H, Jiang WR, Robledo N, Leveque V, Ali S, et al. (2007) Characterization of the metabolic activation of hepatitis C virus nucleoside inhibitor beta-D-2′-Deoxy-2′-fluoro-2′-C-methylcytidine (PSI-6130) and identification of a novel active 5′-triphosphate species. J Biol Chem 282: 29812–29820.
24. Murakami E, Bao H, Ramesh M, McBrayer TR, Whitaker T, et al. (2007) Mechanism of activation of beta-D-2′-deoxy-2′-fluoro-2′-c-methylcytidine and inhibition of hepatitis C virus NS5B RNA polymerase. Antimicrob Agents Chemother 51: 503–509.
25. Moradpour D, Evans MJ, Gosert R, Yuan Z, Blum HE, et al. (2004) Insertion of green fluorescent protein into nonstructural protein 5A allows direct visualization of functional hepatitis C virus replication complexes. J Virol 78: 7400–7409.
26. Masaki T, Suzuki R, Saeed M, Mori K, Matsuda M, et al. (2010) Production of infectious hepatitis C virus by using RNA polymerase I-mediated transcription. J Virol 84: 5824–5835.
27. Shi ST, Lee KJ, Aizaki H, Hwang SB, Lai MMC (2003) Hepatitis C Virus RNA Replication Occurs on a Detergent-Resistant Membrane That Cofractionates with Caveolin-2. J Virol 77: 4160–4168.
28. Gosert R, Egger D, Lohmann V, Bartenschlager R, Blum HE, et al. (2003) Identification of the Hepatitis C Virus RNA Replication Complex in Huh-7 Cells Harboring Subgenomic Replicons. J Virol 77: 5487–5492.
29. Palmer AE, Jin C, Reed JC, Tsien RY (2004) Bcl-2-mediated alterations in endoplasmic reticulum Ca2+ analyzed with an improved genetically encoded fluorescent sensor. Proc Natl Acad Sci U S A 101: 17404–17409.
30. Dittmer PJ, Miranda JG, Gorski JA, Palmer AE (2009) Genetically encoded sensors to elucidate spatial distribution of cellular zinc. J Biol Chem 284: 16289–16297.
31. Nomaguchi M, Ackermann M, Yon C, You S, Padmanbhan R (2003) De Novo Synthesis of Negative-Strand RNA by Dengue Virus RNA-Dependent RNA Polymerase In Vitro: Nucleotide, Primer, and Template Parameters. J Virol 77: 8831–8842.
32. Klumpp K, Ford MJ, Ruigrok RW (1998) Variation in ATP requirement during influenza virus transcription. J Gen Virol 79(Pt 5): 1033–1045.
33. Vreede FT, Gifford H, Brownlee GG (2008) Role of initiating nucleoside triphosphate concentrations in the regulation of influenza virus replication and transcription. J Virol 82: 6902–6910.
34. Frick DN, Lam AM (2006) Understanding helicases as a means of virus control. Curr Pharm Des 12: 1315–1338.
35. Gurer C, Hoglund A, Hoglund S, Luban J (2005) ATPgammaS disrupts human immunodeficiency virus type 1 virion core integrity. J Virol 79: 5557–5567.
36. Li PP, Itoh N, Watanabe M, Shi Y, Liu P, et al. (2009) Association of simian virus 40 vp1 with 70-kilodalton heat shock proteins and viral tumor antigens. J Virol 83: 37–46.
37. Dennis PB, Jaeschke A, Saitoh M, Fowler B, Kozma SC, et al. (2001) Mammalian TOR: a homeostatic ATP sensor. Science 294: 1102–1105.
38. Zamaraeva MV, Sabirov RZ, Maeno E, Ando-Akatsuka Y, Bessonova SV, et al. (2005) Cells die with increased cytosolic ATP during apoptosis: a bioluminescence study with intracellular luciferase. Cell Death Differ 12: 1390–1397.
39. Berg J, Hung YP, Yellen G (2009) A genetically encoded fluorescent reporter of ATP:ADP ratio. Nat Methods 6: 161–166.
40. Niwa H, Yamamura K, Miyazaki J (1991) Efficient selection for high-expression transfectants with a novel eukaryotic vector. Gene 108: 193–199.
41. Soga T, Ohashi Y, Ueno Y, Naraoka H, Tomita M, et al. (2003) Quantitative metabolome analysis using capillary electrophoresis mass spectrometry. J Proteome Res 2: 488–494.
42. Haraguchi T, Shimi T, Koujin T, Hashiguchi N, Hiraoka Y (2002) Spectral imaging fluorescence microscopy. Genes Cells 7: 881–887.
43. Ishii M, Ikushima M, Kurachi Y (2005) In vivo interaction between RGS4 and calmodulin visualized with FRET techniques: possible involvement of lipid raft. Biochem Biophys Res Commun 338: 839–846.
44. Murakami K, Kimura T, Osaki M, Ishii K, Miyamura T, et al. (2008) Virological characterization of the hepatitis C virus JFH-1 strain in lymphocytic cell lines. J Gen Virol 89: 1587–1592.
45. Inoue Y, Aizaki H, Hara H, Matsuda M, Ando T, et al. (2011) Chaperonin TRiC/CCT participates in replication of hepatitis C virus genome via interaction with the viral NS5B protein. Virology 410: 38–47.
46. Taguwa S, Kambara H, Omori H, Tani H, Abe T, et al. (2009) Cochaperone activity of human butyrate-induced transcript 1 facilitates hepatitis C virus replication through an Hsp90-dependent pathway. J Virol 83: 10427–10436.
47. Takeuchi T, Katsume A, Tanaka T, Abe A, Inoue K, et al. (1999) Real-time detection system for quantification of hepatitis C virus genome. Gastroenterology 116: 636–642.

- 670 -

ORIGINAL ARTICLE

# Replication and infectivity of a novel genotype 1b hepatitis C virus clone

Tomoko Date[1], Kenichi Morikawa[1,2,†], Yasuhito Tanaka[3], Keiko Tanaka-Kaneko[4], Tetsutaro Sata[4,‡], Masashi Mizokami[5] and Takaji Wakita[1]

Departments of [1]Virology II and [4]Pathology, National Institute of Infectious Diseases, 1-23-1 Toyama, Shinjuku, Tokyo 162-8640, [2]Division of Gastroenterology, Department of Medicine, Showa University School of Medicine, 1-5-8 Hatanodai, Shinagawa-ku, Tokyo 142-8666, [3]Department of Virology & Liver Unit, Nagoya City University Graduate School of Medical Sciences, Kawasumi, Mizuho, Nagoya 467-8601, and [5]The Research Center for Hepatitis and Immunology, National Center for Global Health and Medicine, 1-7-1 Kounodai, Ichikawa 272-8516, Japan

## ABSTRACT

Hepatitis C virus infection is a major public health problem because of an estimated 170 million carriers worldwide. Genotype 1b is the major subtype of HCV in many countries and is resistant to interferon therapy. Study of the viral life cycle is important for understanding the mechanisms of interferon resistance of genotype 1b HCV strains. For such studies, genotype 1b HCV strains that can replicate and produce infectious virus particles in cultured cells are required. In the present study, we isolated HCV cDNA, which we named the NC1 strain, from a patient with acute severe hepatitis. Subgenomic replicon experiments revealed that several mutations enhanced the colony-formation efficiency of the NC1 replicon. The full-length NC1 genome with these adaptive mutations could replicate in cultured cells and produce infectious virus particles. The density gradient profile and morphology of the secreted virus particles were similar to those reported for the JFH-1 virus. Further introduction of a combination of mutations of the NS3 and NS5a regions into the NC1 mutants further enhanced secreted core protein levels and infectious virus titers in the culture medium of HCV-RNA-transfected cells. However, the virus infection efficiency was not sufficient for autonomous virus propagation in cultured cells. In conclusion, we established a novel cell culture-adapted genotype 1b HCV strain, termed NC1, which can produce infectious virus when the viral RNA is transfected into cells. This system provides an important opportunity for studying the life cycle of the genotype 1b HCV.

**Key words**  genotype 1b, hepatitis C virus (HCV), replicon, virus culture.

Hepatitis C virus infection leads to chronic liver diseases including cirrhosis and hepatocellular carcinoma, and is a major public health problem because of an estimated 170 million carriers worldwide (1–3). HCV is a plus-strand RNA virus that displays marked genetic heterogeneity and is currently classified into six major genotypes (4). Some HCV genotypes display regional distribution, although genotypes 1 and 2 occur worldwide. Genotype 1b is the major subtype in Japan, whereas genotype 2a is the most common minor subtype (5). Infection with genotype 1b HCV is known to be resistant to interferon therapy, whereas infection with genotype 2a is

1

usually sensitive to such intervention (6). Current standard therapy for HCV-related chronic hepatitis is based on a combination of IFN and ribavirin, although virus eradication rates are limited to approximately 50% for genotype 1b HCV infection (7–9). PI have been approved for clinical use against HCV infection in the USA, Europe and Japan, and triple combination therapy that includes PI is expected to improve treatment efficacy. However, the development of other anti-HCV drugs with different modes of action is important to achieve greater efficacy and to avoid the emergence of drug-resistant viruses. To that end, a detailed understanding of the viral replication mechanism is needed to identify novel antiviral targets.

Although HCV belongs to the *Flaviviridae* family and has a genome structure similar to the other flaviviruses, efficient virus propagation in cultured cells has been difficult ever since the discovery of the virus (10). A subgenomic HCV-RNA replicon system was developed using the genotype 1b Con1 strain (11), which enabled the assessment of HCV replication in cultured cells. Subsequently, the genotype 2a JFH-1 strain was cloned and a HCV culture system was established using this strain (12–14). However, such efficient virus production could not be reproduced using genotype 1b HCV strains, even when adaptive mutations were introduced to enhance their replication efficiency in cultured cells (15). Thus, it remains necessary to obtain genotype 1b HCV strains that can replicate and produce infectious virus particles in cultured cells.

In the present study, we isolated HCV cDNA, which we named the NC1 strain, from a patient with acute severe hepatitis. In a subgenomic replicon experiment using the NC1 clone, we found several mutations that enhanced colony-formation efficiency of the NC1 replicon. Interestingly, the full-length NC1 genome with these adaptive mutations could replicate in cultured cells and produce infectious virus particles. However, the viral infection efficiency was not sufficient for autonomous virus propagation in cultured cells even though virus production efficiency could be increased by the introduction of multiple mutations into the virus genome.

## MATERIALS AND METHODS

### Cell culture system

Huh7 and Huh7.5.1 cells (a generous gift from Dr Francis V. Chisari) were cultured in 5% CO$_2$ at 37°C in DMEM containing 10% fetal bovine serum (DMEM-10) (13, 16).

### HCV clones

The genotype 1b HCV clone NC1 was isolated from a patient with acute severe hepatitis (prothrombin

time <40%). The patient was a 48-year-old woman who had no history of blood transfusions. Total RNA was extracted from the serum during the acute phase, and HCV cDNA covering the entire genome was amplified by RT-PCR using HCV-specific primers (S-Table 1). All amplified products were purified and then cloned into pGEM-T EASY™ vectors (Promega, Madison, WI, USA). PCR products and plasmids were sequenced using HCV-specific primer sets (S-Table1), a Big Dye Terminator Mix and an automated DNA sequencer (PE Biosystems, Foster City, CA, USA). Based on the consensus sequence of the NC1 strain, we then assembled pNC1 (DDBJ/EMBL/GenBank accession number: AB691953), which contained the full-length NC1 cDNA downstream of the T7 RNA polymerase promoter. An NC-1 subgenomic replicon construct, pSGR-NC1, was also assembled according to previously published methods used for Con1 replicon and pSGR-JFH1 construction (10, 17). The first 213 nucleotides at the NS3 region of pSGR-NC1 are identical with the Con1 sequence because of the restriction site used for plasmid construction. Several mutations were introduced into the pNC1 and pSGR-NC1 constructs as reported previously using specific primer sets (S-Table 2) (17). pNC1/wt contained the wild-type sequence of the NC1 strain. pNC1/SY and pNC1/SG contained S2197Y and S2204G mutations, respectively. pNC1/EGSY contained both E1202G and S2197Y mutations. pNC1/KTSY contained both K1846T and S2197Y mutations. pNC1/EGKTSY contained the three mutations, E1202G, K1846T and S2197Y.

### Subgenomic replicon assay

Subgenomic replicon RNA was synthesized as reported previously (17). The synthesized replicon RNA (3 μg) was adjusted to a total RNA amount of 10 μg using cellular RNA isolated from non-transfected Huh7 cells and was then electroporated into naive Huh7 and Huh 7.5.1 cells as reported previously (17). G418 (1 mg/mL) was added to the culture medium for 3 weeks, and drug-resistant colonies were fixed with buffered formalin and stained with crystal violet or were cloned for further analysis. For the cloning analysis of the replicon cells, G418-resistant colonies were isolated by using cloning cylinders (Asahi Techno Glass Co., Tokyo, Japan) and were expanded until they reached 80% to 90% confluency in 10-cm diameter dishes. Total RNA was extracted from the cloned G418-resistant cells by using the ISOGEN reagent (Nippon Gene, Tokyo, Japan), and the replicon RNA was quantified using real-time detection RT-PCR (RTD-PCR) as reported previously (18). The cDNAs of the HCV-RNA replicon were synthesized and then amplified by PCR. The sequence of each replicon was determined (17).

## Full-length HCV-RNA transfection

Full-length HCV-RNA was synthesized from pNC1 and its derivatives that contained adaptive mutations as described previously (12, 19, 20). Synthesized HCV-RNA (10 $\mu$g) was transfected into Huh7.5.1 cells. The HCV core protein level in the culture supernatant was measured using Lumipulse Ortho HCV Ag (Ortho-Clinical Diagnostics, Tokyo, Japan) (21), and infectivity of the supernatant was determined by measurement of its focus-formation efficiency (13, 19). In some experiments, the transfected cell pellet was harvested and dissolved with RIPA buffer containing 0.1% SDS. HCV core protein levels in cell lysates were also measured using the Lumipulse Ortho HCV Ag.

## Density gradient analysis of secreted virus particles

Culture medium (1 mL) derived from transfected cells was harvested for density gradient analysis 2 or 15 days after transfection of full-length NC1/SY HCV RNA. The cleared culture medium was layered onto a stepwise sucrose gradient (60% [wt/vol] to 10%) and centrifuged for 16 hrs in an SW41 rotor (Beckman, Palo Alto, CA, USA) at 200,000 $\times$ g at 4°C. After centrifugation, 18 fractions were harvested from the bottom of the tubes. The core protein concentration in each fraction was determined by analysis of 100 $\mu$L of each fraction.

## Electron microscopy

Culture medium (150 mL) containing NC1/SY virus particles were collected from the cells 15 days after transfected cells. The collected culture medium was ultrafiltrated and concentrated 20-fold using a pellicon-2 filter system (Millipore, Bedford, MA, USA). The sample was layered onto a stepwise sucrose gradient (60% [wt/vol] to 10%) and centrifuged for 4 hrs in an SW28 rotor (Beckman, Palo Alto, CA, USA) at 140,000 $\times$ g at 4°C. Thereafter, fractions were harvested from the bottom of the tubes. The core protein concentration in each fraction was determined and the fraction with the highest core protein level was ultrafiltrated for electron microscopic analysis. To visualize HCV particles, we adsorbed the purified virus samples onto carbon-coated grids for 1 min. The grids were then stained with 1% uranyl acetate for 1 min and examined under an H-7650 transmission electron microscope (Hitachi High-Technologies Co., Tokyo, Japan) (22).

## Human hepatocyte chimeric mice experiments

Human hepatocytes were transplanted into uPA$^{+/+}$/SCID$^{+/+}$ mice as described previously (23, 24). These mice were obtained from Phoenix Bio Co., Ltd (Hiroshima, Japan). All mice received hepatocyte transplants from the same donor. Human albumin levels in the sera of the mice were monitored to evaluate the percentage replacement of mouse hepatocytes with human hepatocytes in the mouse liver. These human hepatocyte chimeric mice, in which the mouse liver cells were largely (>90%) replaced with human hepatocytes, were used to reduce the potential influence of mouse-derived mRNA on the results obtained. Two mice were each inoculated with purified NC1/SY HCV particles containing 11.6 fmol core protein. The HCV-RNA titer in inoculated mouse serum was monitored by RTD-PCR each week after inoculation.

## RESULTS

### Genotype 1b HCV clone isolated from a patient with acute severe hepatitis

HCV cDNA was isolated from a patient with acute severe hepatitis. This patient was a 48-year-old woman without any history of blood transfusions. She developed acute severe hepatitis as diagnosed by acute liver failure associated with stage I encephalopathy and low serum prothrombin time (<40%). In the patient's serum, no marker of cytomegalovirus, Epstein-Barr virus, herpes simplex virus, hepatitis A virus or hepatitis B virus was detected. However, only HCV-RNA was detected using RT-PCR analysis, and the virus RNA titer in her serum at admission was 16,660 KIU/mL. The genotype 1b HCV sequence was detected by sequencing analysis of the PCR fragment. The patient was therefore diagnosed as suffering from acute severe hepatitis caused by genotype 1b HCV infection. She received IFN-$\alpha$ treatment, which cleared the viral infection, and she subsequently recovered. The entire sequence of the amplified HCV genomic cDNA was then determined and this HCV strain was designated as NC1. The sequencing analysis indicated that this NC1 strain shared 91.2% nucleotide and 94.4% amino acid sequence homology with the Con1 strain.

### Subgenomic replicon analysis of the NC1 strain

To analyze the replication efficiency of the genotype 1b NC1 strain, we constructed the subgenomic replicon, pSGR-NC1, in the form of a Con1 replicon and pSGR-JFH1 (10, 17). This synthesized NC1 replicon RNA was transfected by electroporation into Huh7 or Huh7.5.1 cells. The transfected cells were then grown for 3 weeks in a selection culture that contained 1 mg/mL G418. Several colonies survived this selection culture, as illustrated by crystal violet staining (Fig. 1). The

3

T. Date *et al.*

## a

pSGR-NC1



## b
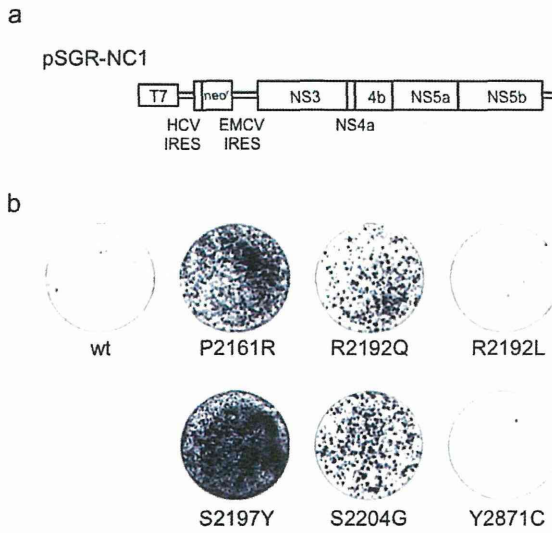


**Fig. 1.  NC1 subgenomic HCV replicon construct and colony formation of NC1 replicon RNA-transfected Huh7 cells.** (a) Organization of the subgenomic replicon construct pSGR-NC1. Open reading frames (wide boxes) are flanked by untranslated regions (narrow boxes). The T7 RNA promoter is located upstream of the 5' end of the replicon construct. (b) Subgenomic RNAs were synthesized *in vitro* using pSGR-NC1 (wt) and replicon constructs containing one of the mutations P2161R, R2192Q, R2192L, S2197Y, S2204G and Y2871C as templates. Transcribed subgenomic replicon RNAs (3 $\mu$g each) were electroporated into Huh7 cells and the cells were cultured with G418 for 3 weeks before staining with crystal violet. Experiments were carried out in triplicate and representative staining examples are shown.

colony-formation efficiency of the NC1 replicons was 1.77 $\pm$ 1.54 CFU/$\mu$g RNA, which was lower than the colony-formation efficiency of the JFH-1 subgenomic replicon that was determined in our previous study (5.32 $\pm$ 5.02 $\times$ 10$^4$ CFU/$\mu$g RNA) (17). Six colonies of the transfected Huh7 cells and 14 colonies of the transfected Huh7.5.1 cells were cloned and expanded for further analysis. Replicon RNA was isolated from each replicon cell clone, and the HCV-RNA titer and sequence of the replicon genome were determined (Table 1). The average HCV-RNA titers in the replicon cell clones derived from Huh7 and Huh7.5.1 cells were determined by RTD-PCR as 4.28 $\pm$ 3.43 $\times$ 10$^6$ and 6.72 $\pm$ 7.14 $\times$ 10$^6$ copies/$\mu$g RNA, respectively.

We next determined the sequence of the replicating replicon genome in each replicon transfected cell clone. All of the clones had at least one non-synonymous mutation and three clones also had a synonymous mutation (Table 1). We found non-synonymous mutations in all of the subgenomic non-structural regions of the replicon genome, and five of the mutations were found in more than one replicon genomic clone. Thus, of the mutations found in the NS5A region, P2161R, R2192L and

**Table 1.** Mutations and RNA titer of the NC1 replicon cell clones

| Replicon clones† | nt mutation | nt position‡ | aa mutation | aa position§ | Region | Replicon RNA titer |
|---|---|---|---|---|---|---|
| 2 | G>A | 5302(6916) | R>Q | 2192 | NS5a | 3.58E+05 |
|  | T>Y | 5490(7104) | S>S,P | 2255 | NS5a |  |
| 5 | G>R | 4046(5660) | none |  | NS4b | 1.56E+07 |
|  | A>G | 4088(5702) | I>M | 1787 | NS4b |  |
|  | C>A | 5317(6931) | S>Y | 2205 | NS5a |  |
|  | C>S | 6579(8193) | Q>Q,E | 2618 | NS5b |  |
| 2–1 | T>C | 3965(5579) | none |  | NS4b | 3.17E+05 |
|  | T>G | 5346(6960) | S>A | 2207 | NS5a |  |
| 2–2 | C>G | 5209(6823) | P>R | 2161 | NS5a | 8.16E+06 |
| 2–3 | T>C | 1721 | none |  | E-I †† | 3.97E+06 |
|  | C>A | 4855(6469) | S>Y | 2043 | NS5a |  |
| 2–5 | T>C | 3694(5308) | V>C | 1656 | NS3 | 1.80E+07 |
|  | C>G | 5209(6823) | P>R | 2161 | NS5a |  |
| 2–7 | G>T | 5302(6916) | R>L | 2192 | NS5a | 2.91E+06 |
| 2–8 | T>C | 5067(6681) | C>R | 2114 | NS5a | 1.98E+06 |
|  | A>G | 7339(8953) | Y>C | 2871 | NS5b |  |
| 2–9 | C>A | 5317(6931) | S>Y | 2197 | NS5a | 1.58E+07 |
| 2–10 | A>G | 5287(6901) | K>R | 2187 | NS5a | 1.90E+07 |
|  | A>G | 5337(6951) | S>G | 2204 | NS5a |  |
|  | A>G | 7339(8953) | Y>C | 2871 | NS5b |  |
| 2–11 | C>A | 584 | D>E |  | NEO | 2.50E+06 |
|  | A>T | 3762(5376) | S>C | 1679 | NS4a |  |
|  | T>A | 5248(6862) | M>K | 2174 | NS5a |  |
| 2–12 | C>T | 5291(6905) | none |  | NS5a | 1.02E+06 |
|  | G>T | 5302(6916) | R>L | 2192 | NS5a |  |
| 2–13 | C>A | 4850(6464) | N>K | 2041 | NS5a | 3.65E+06 |
| 2–15 | C>T | 5299(6913) | A>V | 2191 | NS5a | 8.07E+05 |
|  | A>G | 5337(6951) | S>G | 2204 | NS5a |  |
|  | A>G | 6014(7628) | none |  | NS5b |  |
|  | A>G | 6015(7629) | I>V | 2430 | NS5b |  |
| H1 | C>A | 5301(6915) | none |  | NS5a | 1.01E+07 |
|  | C>A | 5317(6931) | S>Y | 2197 | NS5a |  |
| H3 | G>A | 661 | G>E |  | NEO | 4.77E+06 |
|  | C>A | 5323(6937) | A>D | 2199 | NS5a |  |
| H6 | C>A | 5265(6879) | H>N | 2180 | NS5a | 1.21E+06 |
| H7 | C>A | 5308(6922) | S>Y | 2194 | NS5a | 4.53E+05 |
| H10 | C>A | 5317(6931) | S>Y | 2197 | NS5a | 5.12E+06 |
| H12 | A>C | 5325(6939) | S>R | 2200 | NS5a | 4.03E+06 |

†Replicon clones 2~2–15 were derived from Huh7.5.1 cells, and the H1~H12 replicon clones were derived from Huh7 cells. ‡Position within the subgenomic replicon and within full-length NC1 (in parentheses).
§Position within the complete open reading frame of full-length NC1.
¶Copy/$\mu$g RNA. ††E-I, EMCV-IRES.

S2204G mutations were independently detected in two different replicon cell clones, and the S2197Y mutation was detected in three different replicon cell clones. In addition, R2192 was not only mutated to R2192L but was also found as an R2192Q mutation in one replicon. The Y2871C mutation in NS5B was detected in two different replicon cell clones. We therefore selected P2161R, R2192L, R2192Q, S2197Y, S2204G and Y2871C mutations for further analysis to determine their adaptive effects. We inserted P2161R, R2192L, R2192Q, S2197Y, S2204G and Y2871C mutations into the pSGR-NC1 genome and tested

**4**

the colony-formation efficiency of the mutant replicons. As shown in Figure 1b, P2161R, R2192Q, S2197Y and S2204G mutations had adaptive effects for colony formation. However, R2192L and Y2871C mutations did not enhance colony-formation efficiency.

## Full-length HCV replication

As shown above, some of the mutations detected in the NC1 subgenomic replicon that was transfected into cells exhibited adaptive effects that increased colony-formation efficiency. We next determined whether full-length NC1 HCV clones with these mutations were able to replicate in cultured cells and to produce infectious virus. We therefore introduced the same six mutations that we tested in the subgenomic replicon assay into the full-length NC1 HCV cDNA (Fig. 2a). Full-length viral RNA was synthesized from linearized pNC1 and its mutant derivatives and was electroporated into Huh7.5.1 cells. All of the transfected cells were serially passaged, and HCV core protein levels in the culture supernatant were monitored over time (Fig. 2b). Interestingly, only cells transfected with the NC1 HCV-RNA with an S2197Y or S2204G mutation secreted a significant amount of HCV core protein into the culture medium. Secreted HCV core protein levels reached a maximum at 5–10 days post- transfection and subsequently continuously decreased in the culture medium of the cells transfected with the viral RNA containing S2197Y or S2204G mutation until 32 days after transfection. This reduction in HCV core protein levels after a certain number of cell passages was reproducible and was confirmed in repeated experiments.

## Characterization of the NC1 virus particles secreted from NC1 RNA-transfected cells

Of the six NC1 constructs with mutations that were transfected into cells, transfection of NC1/SY RNA, which had the S2197Y mutation, resulted in secretion of the highest level of HCV core protein into the culture medium (Fig. 2b). We therefore further analyzed the HCV particles produced from NC1/SY RNA-transfected cells. Synthesized NC1/SY RNA was transfected again into Huh7.5.1 cells, the transfected cells were passaged and the culture medium was harvested at cell passaging. HCV core protein levels were relatively high in the culture medium from the NC1/SY RNA-transfected cells on days 2 and 15 post-transfection (Table 2). Infectivity of the culture medium was also detected at both time points, although at very low levels (Table 2). We also analyzed HCV core protein in the culture media obtained at these two time points using a density gradient assay. Both media exhibited a high, narrow peak of HCV core protein in fraction 9, which had a density of 1.15 g/mL, as well as a broader
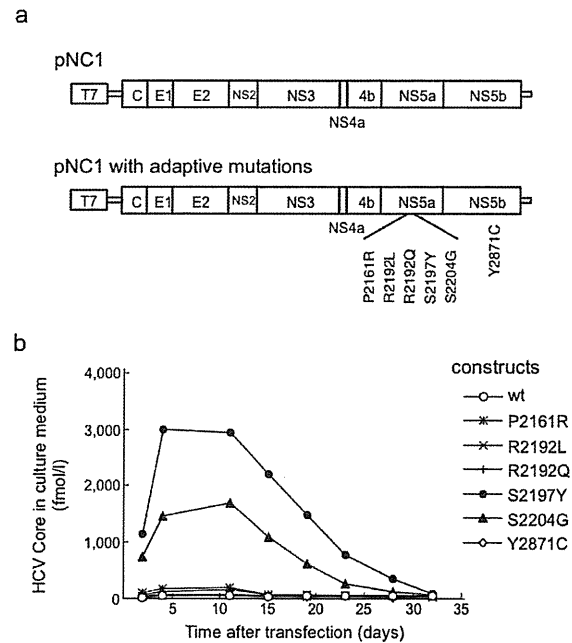


**Fig. 2. Analysis of the HCV core protein released into the cell culture medium after transfection of NC1 full-length HCV-RNA.** (a) Organization of the full-length NC1construct, pNC1 (upper). Open reading frames (wide boxes) are flanked by untranslated regions (narrow boxes). A T7 RNA promoter is located upstream of the 5′ end of the HCV cDNA construct. Six of the mutations identified in the replicon cell clones were independently introduced into the pNC1 construct (lower). (b) Huh7.5.1 cells were transfected with RNA transcribed from pNC1 with the wild-type HCV sequence (wt) or with RNA from one of the six constructs containing one of the mutations P2161R, R2192Q, R2192L, S2197Y, S2204G or Y2871C. Two independently transfected cell lines were passaged for each construct. At each time point after transfection, the culture medium was harvested and analyzed for the presence of HCV core protein. Average data of duplicate transfections are indicated.

**Table 2.** HCV core protein and infectivity levels in the culture medium of NC1/SY RNA-transfected cells

| Days post-transfection | HCV Core (fmol/L) | Infectivity (ffu/mL) |
|---|---|---|
| 2 | 1721 | 3 |
| 15 | 1009 | 16 |

minor peak which had a density of 1.02 to 1.04 g/mL (Fig. 3a). Interestingly, these density gradient profiles were quite similar to the previously described profile of JFH-1 (12). We further identified viral particles in the peak fraction of NC1/SY virus particles obtained following density gradient centrifugation by electron microscopic analysis (Fig. 3b). The observed particles exhibited a spherical shape with diameters of approximately 50–55 nm.

5

a



b
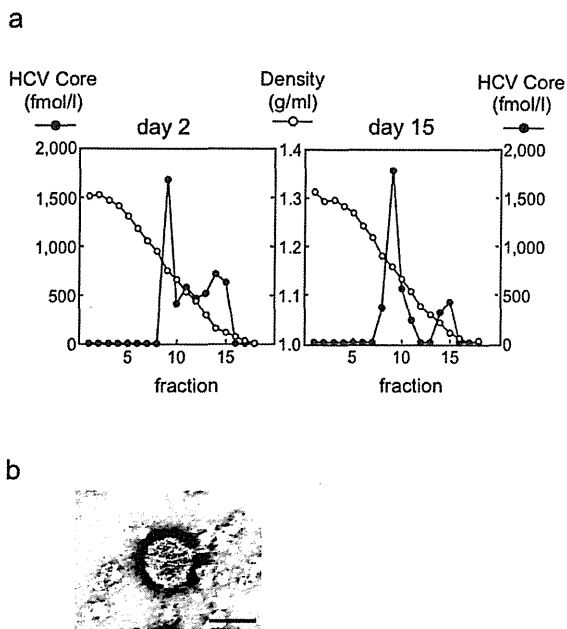


**Fig. 3. Characterization of secreted HCV particles from NC1/SY RNA-transfected cells.** (a) Sucrose density gradient analysis of the culture supernatant from NC1/SY RNA-transfected Huh7.5.1 cells. One ml of the culture supernatant of transfected cells that was collected on day 2 and day 15 post-transfection (Table 2) was cleared by centrifugation and filtration. Each supernatant was overlaid on a stepwise sucrose density gradient (0, 10, 20, 30, 40, 50 and 60% sucrose) and centrifuged for 16 hrs at 200,000 × $g$ at 4°C. Eighteen fractions were collected from the bottom of the tubes and the concentration of HCV core protein in each fraction was determined. Closed and open circles indicate HCV core protein levels (fmol/L) and the sucrose density (g/mL) of the fractions, respectively. (b) Negative-stained HCV particles were observed by electron microscopy. NC1/SY virus particles were purified from the culture medium at 15 days post-transfection and observed by electron microscopy using negative staining. Scale bar, 50 nm.

## Infectivity of the NC1/SY virus in human hepatocyte-transplanted uPA/SCID mice

We next determined the *in vivo* infectivity of the NC1/SY virus using human hepatocyte-transplanted uPA/SCID mice, which were reported to be permissive for HCV infection (23). We harvested cell culture media containing NC1/SY virus at 6 days after RNA transfection and was concentrated approximately 20-fold. The concentrated NC1/SY virus was inoculated into two mice designated as PXB 21–39 and PXB 21–40 (Table 3). Human albumin levels in the sera of the inoculated mice were higher than 3 mg/mL during the experiment, which supported the fact that there was a high level of replacement of mouse hepatocytes with human hepatocytes in the mouse liver. Both mice were negative for HCV-RNA at 1 week after inocula-

**Table 3.** Serum HCV-RNA titer in human hepatocyte chimeric mice inoculated with the NC1/SY virus produced in cultured cells

| Days post-infection | Mouse ID† | |
|---|---|---|
| | PXB 21–39 | PXB 21–40 |
| 7 | – | – |
| 14 | + | – |
| 21 | – | – |
| 28 | – | – |
| 35 | – | – |

†Two mice were independently inoculated with 300 $\mu$L NC1/SY (38,600 fmol/L).
+, PCR positive ($<2.1 \times 10^4$ copies/mL); –, PCR negative.

tion (Table 3). The PXB 21–39 mouse became transiently HCV-RNA positive only at 2 weeks post-inoculation but thereafter remained negative from 3 to 5 weeks post-inoculation. The PXB 21–40 mouse remained HCV-RNA negative until 5 weeks post-inoculation. Thus, the cell culture-adapted NC1/SY virus in the inoculum may have possessed *in vivo* infectivity although this infectivity was at a low level.

## Combinatory effects of adaptive mutations in different regions

The above experiment showed that NC1/SY RNA-transfected cells could produce infectious virus particles but at very low efficiency. To increase the replication and virus production efficiency of the NC1/SY virus, we tested the effect of introducing additional adaptive mutations into NC1. Thus, the E1202G mutation in NS3 (25) and/or the K1846T mutation in NS4B (26) were introduced into pNC1/SY (Fig. 4a) yielding pNC1/EGSY, pNC1/KTSY and pNC1/EGKTSY. RNAs transcribed from these synthesized constructs were transiently transfected into Huh7.5.1 cells. In this transient transfection experiment, NC1/EGSY and NC1/EGKTSY-RNA-transfected cells expressed higher levels of HCV core protein both in the culture medium and in the cell lysate from 48 to 96 hrs after transfection than cells transfected with RNA of the other NC1 mutants (Fig. 4b and c). However, the NC1/KTSY RNA-transfected cells expressed a similar level of HCV core protein as that expressed by NC1/SY. Interestingly, the E1202G mutation not only increased the level of the HCV core protein but also the infectivity of the culture medium. At 3 days post-transfection, HCV core protein levels reached a concentration of 8193 fmol/L in the medium of NC1/EGSY RNA-transfected cells, and, at the same time point, the infectivity titer in the culture medium of these cells reached 792 ffu/mL (Fig. 4b and Table 4). However, by 25 days post-transfection, the

**6**

## a

**pNC1 with adaptive mutations**



## b



## c
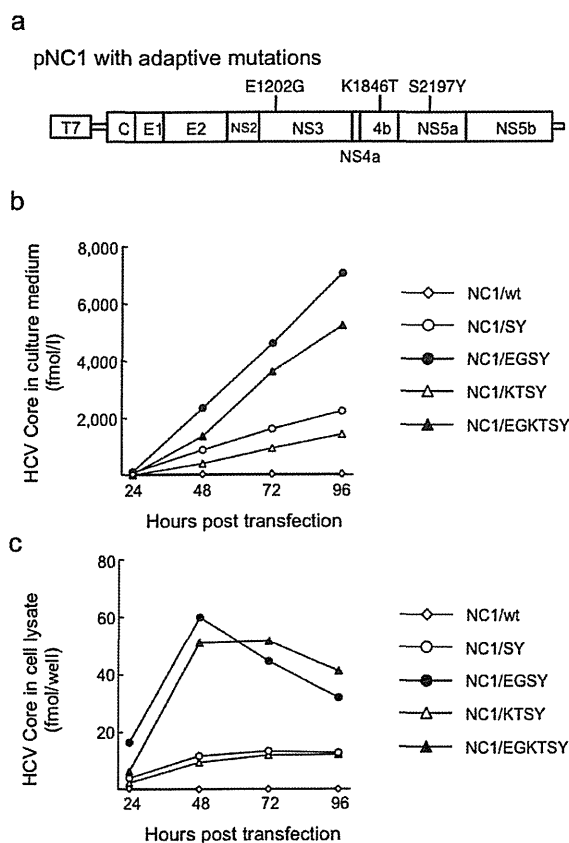


**Fig. 4. Kinetics of HCV core protein release into the culture medium and cellular HCV protein expression.** (a) Position of the E1202G and K1846T mutations, which were introduced alone or in combination into the full-length pNC1 containing the S2197Y mutation, is shown. Transcribed full-length HCV-RNAs from pNC1 and its mutated derivatives were transfected into Huh7 cells. At each time point, the culture medium and an aliquot of transfected cells were harvested. HCV core protein levels in the culture medium (b) and the cell lysate (c) were determined as described in Materials and Methods. Data indicate the average core protein concentration from two independent transfections. wt, wild type; EG, E1202G; KT, K1846T; SY, S2197Y.

infectivity titer in the culture medium of the NC1/EGSY RNA-transfected cells had decreased to 23.3 ffu/mL. Furthermore, reinfection of the secreted virus did not result in productive infection.

## DISCUSSION

In previous studies, we isolated a cell culture infectious genotype 2a HCV strain, the JFH-1 strain, from a patient with fulminant hepatitis (12, 27). In the present study, we isolated a novel genotype 1b HCV cDNA, the NC1 strain. We tested NC1 strain replication efficiency in cultured cells using a drug-selectable subgenomic replicon

**Table 4.** HCV core protein levels in, and infectivity of, the culture medium of NC1 RNA-transfected cells

| Days post-transfection | HCV construct | HCV core (fmol/L) | Infectivity (ffu/mL) |
|---|---|---|---|
| 3 | NC1/SY | 2468 | 23.3 |
|  | NC1/EGSY | 8193 | 792.0 |
|  | NC1/KTSY | 1079 | 3.3 |
|  | NC1/EGKTSY | 5064 | 467.0 |
| 25 | NC1/SY | 963 | 3.3 |
|  | NC1/EGSY | 515 | 23.3 |
|  | NC1/KTSY | 319 | 0.0 |
|  | NC1/EGKTSY | 995 | 6.7 |

assay. Although the colony-forming efficiency of the NC1 replicon was lower than that of JFH-1, we still isolated multiple NC1 replicon cell clones. This result suggested that adaptive mutations in the replicon genome were necessary for efficient replication and that clones that expressed neomycin-resistant gene products were selected. Indeed, some mutations were identified in the NC1 replicon that enhanced colony-formation efficiency (Fig. 1). Notably, the S2197Y and S2204G mutations also increased core protein secretion from cells transfected with full-length NC1 HCV-RNA (Fig. 2). The culture medium of the NC1/SY RNA-transfected cells showed marginal infectivity for naive Huh7.5.1 cells. The *in vivo* infectivity of the NC1/SY virus was confirmed by its inoculation into human hepatocyte-transplanted uPA/SCID mice. Although the *in vivo* NC1/SY virus infectivity was very weak and transient, it was detected in one of the two inoculated mice. By introducing additional adaptive mutations into the NC1/SY virus, we found that a combination of E1202G and S2197Y mutations further enhanced HCV replication and virus production in RNA-transfected cells.

HCV was discovered as a causative agent of non-A, non-B hepatitis in 1989 (1, 2). Since then, efforts to understand the viral life cycle of HCV and to identify effective antiviral agents have been hampered by the lack of an efficient cell culture system for this virus. There have already been many attempts to develop a system for HCV infection and replication in cell culture (reviewed in ref 10). However, the viral replication efficiencies reported in these studies were modest, requiring detection by RT-PCR.

We previously isolated an HCV clone, JFH-1, from a fulminant hepatitis patient with HCV (27). A JFH-1-derived subgenomic replicon proved capable of highly efficient replication in a variety of cell lines (17), and produced infectious HCV particles in Huh7 cells (12–14). The development of an HCV infection system using the JFH-1 strain has contributed to our understanding of this important virus. A genotype 1a strain, H77S, which contained five adaptive mutations, was reported to produce infectious

7

T. Date *et al.*

virus following transfection of its synthesized RNA into Huh7 cells (28). It is thus clear that JFH-1 is not the only HCV strain that can be propagated in cultured cells. However, it is also important to understand why JFH-1 is the only strain that replicates efficiently in cultured cells in the absence of adaptive mutations. In order to understand this characteristic of JFH-1, we analyzed the mechanisms that underlie the efficient replication of the JFH-1 strain (29, 30) and identified important sequence differences in the JFH-1 strain compared to the J6CF strain. However, introduction of mutations that would abrogate such sequence differences did not enable efficient replication of genotype 1b HCV strains. These data suggested that it is necessary to identify different mutations that would increase the virus production efficiency of genotype 1b HCV. Further analysis of JFH-1 genomic replication mechanisms may help to determine other differences between the replication of JFH-1 and other strains.

Previous reports have indicated that adaptive mutations enhance viral RNA replication at the expense of virus particle formation efficiency (31). A highly cell culture-adapted Con1 strain can replicate in cultured cells, but it cannot produce infectious virus particles. In the present study, we also attempted to establish a replication-competent genotype 1b HCV strain from a patient with acute severe hepatitis. We identified several adaptive mutations in colony-forming experiments using a subgenomic replicon of this NC1 strain. Notably, S2197Y and S2204G mutations exhibited an adaptive effect for both virus replication and virus particle secretion. The adaptive mutations at amino acid positions 2197 and 2204 were previously reported in genotype 1a and 1b replicon studies (reviewed in ref 32). Although the S2197Y mutation enabled the NC1 strain to produce infectious virus, the infection efficiency of this virus was very weak. We therefore hypothesized that it may be necessary to increase replication efficiency by introducing additional mutations that would facilitate efficient virus production. For this purpose, we introduced and tested the effect of introduction of the previously reported mutations, E1202G in NS3 (25) and K1846T in NS4B (26), into the pNC1/SY construct. Interestingly, virus core protein secretion of NC1/SY was enhanced by introduction of the E1202G mutation but not by introduction of the K2864T mutation. This result suggested that the selection and combination of adaptive mutations is very important for establishment of an infectious genotype 1b HCV strain. Although NC1/EGSY RNA-transfected cells produced high levels of HCV core protein into the culture medium with infectivity, not all of the cells were infected with the virus and viral infection did not continue as the cells were passaged. After several cell passages, only a small number of the transfected cells remained infected (data not shown). This result may be due to a low degree of infection efficiency that was not sufficient for productive infection or may be due to some other unknown mechanisms.

The *in vivo* infectivity of the NC1/SY virus was tested using the human hepatocyte-transplanted uPA/SCID mouse system. The NC1/SY virus showed only transient viremia in one out of two inoculated mice. Interestingly, a highly adapted Con1 strain was previously shown not to be infectious for chimpanzees, whereas a moderately adapted Con1 was infectious. However, the virus recovered from the infected animal was wild-type Con1 virus (33). This result clearly suggests that HCV strains with low replication efficiency are favorable for *in vivo* infection. A wild-type virus with low replication capacity is likely to evade the host immune surveillance system and thereby survive in an *in vivo* situation. However, the JFH-1 virus was infectious not only for cultured cells but also for chimpanzees and human liver-transplanted mice (12, 34, 35). It is therefore important to analyze how HCV can evade host defense mechanisms to understand the mechanism of persistent viral infection. Further detailed studies are necessary for such analysis.

In the present study, we established the cell culture-adapted genotype 1b HCV strain, NC1. Infectious virus was produced from RNA-transfected cells. However, virus infection could not be continuously passaged in Huh7.5.1 cells. Novel antiviral drugs targeting genotype 1b HCV are under development and some of these drugs will be used in a clinical setting. It is likely that such new therapy will be accompanied by the appearance of significant adverse effects and by the emergence of drug-resistant virus. It is therefore important to further develop improved genotype 1b infectious HCV culture systems for future studies so that these problems can be circumvented.

## ACKNOWLEDGMENTS

**8**

Cell culture adapted genotype 1b HCV clone

## DISCLOSURE

None of the authors have any conflicts of interest associated with this study.

## REFERENCES

1. Choo Q.L., Kuo G., Weiner A.J., Overby L.R., Bradley D.W., Houghton M. (1989) Isolation of a cDNA clone derived from a blood-borne non-A non-B viral hepatitis genome. *Science* 244:359–62.
2. Kuo G., Choo Q.L., Alter H.J., Gitnick G.L., Redeker A.G., Purcell R.H., Miyamura T., Dienstag J.L., Alter M.J., Stevens C.E., Tegtmeier G.E., Bonino F., Colombo M., Lee W-S., Kuo C., Berger K., Shuster J.R., Overby L.R., Bradley D.W., Houghton M. (1989) An assay for circulating antibodies to a major etiologic virus of human non-A non-B hepatitis. *Science* 244: 362–4.
3. Kiyosawa K., Sodeyama T., Tanaka E., Gibo Y., Yoshizawa K., Nakano Y., Furuta S., Akahane Y., Nishioka K., Purcell R.H. (1990) Interrelationship of blood transfusion, non-A, non-B hepatitis and hepatocellular carcinoma: analysis by detection of antibody to hepatitis C virus. *Hepatology* 12: 671–5.
4. Bukh J., Purcell R.H., Miller R.H. (1994) Sequence analysis of the core gene of 14 hepatitis C virus genotypes. *Proc Natl Acad Sci USA* 91: 8239–43
5. Ohno T., Mizokami M., Wu R.R., Saleh M.G., Ohba K., Orito E., Mukaide M., Williams R., Lau J.Y. (1997) New hepatitis C virus (HCV) genotyping system that allows for identification of HCV genotypes 1a, 1b, 2a, 2b, 3a, 3b, 4, 5a, and 6a. *J Clin Microbiol* 35: 201–7.
6. Yoshioka K., Kakumu S., Wakita T., Ishikawa T., Itoh Y., Takayanagi M., Higashi Y., Shibata M., Morishima T. (1992) Detection of hepatitis C virus by polymerase chain reaction and response to interferon-alpha therapy: relationship to genotypes of hepatitis C virus. *Hepatology* 16: 293–9.
7. McHutchison J.G., Gordon S.C., Schiff E.R., Shiffman M.L., Lee W.M., Rustgi V.K., Goodman Z.D., Ling M.H., Cort S., Albrecht J.K. (1998) Interferon alfa-2b alone or in combination with ribavirin as initial treatment for chronic hepatitis C. Hepatitis Interventional Therapy Group. *N Engl J Med* 339: 1485–92.
8. Poynard T., Marcellin P., Lee S.S., Niederau C., Minuk G.S., Ideo G., Bain V., Heathcote J., Zeuzem S., Trepo C., Albrecht J. (1998) Randomised trial of interferon alpha2b plus ribavirin for 48 weeks or for 24 weeks versus interferon alpha2b plus placebo for 48 weeks for treatment of chronic infection with hepatitis C virus. International Hepatitis Interventional Therapy Group (IHIT). *Lancet* 352: 1426–32.
9. Di Bisceglie A.M., Hoofnagle J.H. (2002) Optimal therapy of hepatitis C. *Hepatology* 36: S121-7.
10. Bartenschlager R., Lohmann V. (2000) Replication of hepatitis C virus. *J Gen Virol* 81: 1631–48.
11. Lohmann V., Korner F., Koch J., Herian U., Theilmann L., Bartenschlager R. (1999) Replication of subgenomic hepatitis C virus RNAs in a hepatoma cell line. *Science* 285: 110–3.
12. Wakita T., Pietschmann T., Kato T., Date T., Miyamoto M., Zhao Z., Murthy K., Habermann A., Krausslich H.G., Mizokami M., Bartenschlager R., Liang T.J. (2005) Production of infectious hepatitis C virus in tissue culture from a cloned viral genome. *Nat Med* 11:791–6.
13. Zhong J.P., Gastaminza G., Cheng S., Kapadia S., Kato T., Burton D.R., Wieland S.F., Uprichard S.L., Wakita T., Chisari F.V. (2005) Robust hepatitis C virus infection in vitro. *Proc Natl Acad Sci USA* 102:9294–9.
14. Lindenbach B.D., Evans M.J., Syder A.J., Wolk B., Tellinghuisen T.L., Liu C.C., Maruyama T., Hynes R.O., Burton D.R., McKeating J.A., Rice C.M. (2005) Complete replication of hepatitis C virus in cell culture. *Science* 309:623–6.
15. Pietschmann T., Zayas M., Meuleman P., Long G., Appel N., Koutsoudakis G., Kallis S., Leroux-Roels G., Lohmann V., Bartenschlager R. (2009) Production of infectious genotype 1b virus particles in cell culture and impairment by replication enhancing mutations. *PLoS Pathog* 5:e1000475.
16. Akazawa D., Morikawa K., Omi N., Takahashi H., Nakamura N., Mochizuki H., Date T., Ishii K., Suzuki T., Wakita T. (2011) Production and characterization of HCV particles from serum-free culture. *Vaccine* 29:4821–8.
17. Kato T., Date T., Miyamoto M., Furusaka A., Tokushige K., Mizokami M., Wakita T. (2003) Efficient replication of the genotype 2a hepatitis C virus subgenomic replicon. *Gastroenterology* 125:1808–17.
18. Takeuchi T., Katsume A., Tanaka T., Abe A., Inoue K., Tsukiyama-Kohara K., Kawaguchi R., Tanaka S., Kohara M. (1999) Real-time detection system for quantification of hepatitis C virus genome. *Gastroenterology* 116:636–42.
19. Kato T., Date T., Murayama A., Morikawa K., Akazawa D., Wakita T. (2006) Cell culture and infection system for hepatitis C virus. *Nat Protoc* 1:2334–9.
20. Wakita T. (2009) Isolation of JFH-1 strain and development of an HCV infection system. *Methods Mol Biol* 510:305–27.
21. Saeed M., Suzuki R., Kondo M., Aizaki H., Kato T., Mizuochi T., Wakita T., Watanabe H., Suzuki T. (2009) Evaluation of hepatitis C virus core antigen assays in detecting recombinant viral antigens of various genotypes. *J Clin Microbiol* 47:4141–3.
22. Takahashi H., Akazawa D., Kato T., Date T., Shirakura M., Nakamura N., Mochizuki H., Tanaka-Kaneko K., Sata T., Tanaka Y., Mizokami M., Suzuki T., Wakita T. (2010) Biological properties of purified recombinant HCV particles with an epitope-tagged envelope. *Biochem Biophys Res Commun* 395:565–71.
23. Mercer D.F., Schiller D.E., Elliott J.F., Douglas D.N., Hao C., Rinfret A., Addison W.R., Fischer K.P., Churchill T.A., Lakey J.R., Tyrrell D.L., Kneteman N.M. (2001) Hepatitis C virus replication in mice with chimeric human livers. *Nat Med* 7:927–33.
24. Tateno C., Yoshizane Y., Saito N., Kataoka M., Utoh R., Yamasaki C., Tachibana A., Soeno Y., Asahina K., Hino H., Asahara T., Yokoi T., Furukawa T., Yoshizato K. (2004) Near completely humanized liver in mice shows human-type metabolic responses to drugs. *Am J Pathol* 165:901–12.
25. Krieger N., Lohmann V., Bartenschlager R. (2001) Enhancement of hepatitis C virus RNA replication by cell culture-adaptive mutations. *J Virol* 75:4614–24.
26. Lohmann V., Hoffmann S., Herian U., Penin F., Bartenschlager R. (2003) Viral and cellular determinants of hepatitis C virus RNA replication in cell culture. *J Virol* 77:3007–19.
27. Kato T., Furusaka A., Miyamoto M., Date T., Yasui K., Hiramoto J., Nagayama K., Tanaka T., Wakita T. (2001) Sequence analysis of hepatitis C virus isolated from a fulminant hepatitis patient. *J Med Virol* 64:334–9.
28. Yi M., Villanueva R.A., Thomas D.L., Wakita T., Lemon S.M. (2006) Production of infectious genotype 1a hepatitis C virus (Hutchinson strain) in cultured human hepatoma cells. *Proc Natl Acad Sci USA* 103:2310–5.
29. Murayama A., Date T., Morikawa K., Akazawa D., Miyamoto M., Kaga M., Ishii K., Suzuki T., Kato T., Mizokami M., Wakita T.

T. Date *et al.*

(2007) The NS3 helicase and NS5B-to-3'X regions are important for efficient hepatitis C virus strain JFH-1 replication in Huh7 cells. *J Virol* **81**:8030–40.

30. Murayama A., Weng L., Date T., Akazawa D., Tian X., Suzuki T., Kato T., Tanaka Y., Mizokami M., Wakita T., Toyoda T. (2010) RNA polymerase activity and specific RNA structure are required for efficient HCV replication in cultured cells. *PLoS Pathog.* **6**:e1000885.

31. Pietschmann T., Lohmann V., Kaul A., Krieger N., Rinck G., Rutter G., Strand D., Bartenschlager R. (2002) Persistent and transient replication of full-length hepatitis C virus genomes in cell culture. *J Virol* **76**:4008–21.

32. Blight K.J., Norgard E.A. (2006) HCV Replicon Systems. In:Tan SL, editor. *Hepatitis C Viruses: Genomes and Molecular Biology.* Norfolk (UK): Horizon Bioscience; pp. 311–51.

33. Bukh J., Pietschmann T., Lohmann V., Krieger N., Faulk K., Engle R.E., Govindarajan S., Shapiro M., St Claire M., Bartenschlager R. (2002) Mutations that permit efficient replication of hepatitis C virus RNA in Huh-7 cells prevent productive replication in chimpanzees. *Proc Natl Acad Sci USA* **99**:14416–21.

34. Kato T., Choi Y., Elmowalid G., Sapp R.K., Barth H., Furusaka A., Mishiro S., Wakita T., Krawczynski K., Liang T.J. (2008) Hepatitis C virus JFH-1 strain infection in chimpanzees is associated with low pathogenicity and emergence of an adaptive mutation. *Hepatology* **48**:732–40.

35. Lindenbach B.D., Meuleman P., Ploss A., Vanwolleghem T., Syder A.J., McKeating J.A., Lanford R.E., Feinstone S.M., Major M.E., Leroux-Roels G., Rice C.M. (2006) Cell culture-grown hepatitis C virus is infectious in vivo and can be recultured in vitro. *Proc Natl Acad Sci USA* **103**:3805–9

## SUPPORTING INFORMATION

Additional Supporting Information may be found in the online version of this article:

**S-Table 1:** Primers used to amplify and sequence the NC1 HCV strain.

**S-Table 2:** Primers used to introduce mutations into pNC1 and pSGR-NC1.

Please note:Wiley-Blackwell are not responsible for the content or functionality of any supporting materials supplied by the authors. Any queries (other than missing material) should be directed to the corresponding author for the article.

**10**